Cellular/Molecular

A Non-Nuclear NF-κB Modulates Alcohol Sensitivity But Not Immunity

Thilini P. Wijesekera, Zheng Wu, Nicole P. Stephens*, Rahul Godula*, Linda Kao Lew, and Nigel S. Atkinson
Department of Neuroscience and The Waggoner Center for Alcohol and Addiction Research, The University of Texas at Austin, Austin, Texas 78712

NF-κB proteins are well known as transcription factors important in immune system activation. In this highly conserved role, they contribute to changes in behavior in response to infection and in response to a variety of other insults and experiences. In some mammalian neurons, NF-κBs can be found at the synapse and translocate to the nucleus to alter gene expression when activated by synaptic activity. Here, we demonstrate that, in *Drosophila melanogaster*, NF-κB action is important both inside and outside the nucleus and that the *Dif* gene has segregated nuclear and non-nuclear NF-κB action into different protein isoforms. The DifA isoform is a canonical nuclear-acting NF-κB protein that enters the nucleus and is important for combating infection. The DifB variant, but not the DifA variant, is found in the central nervous system (mushroom bodies and antennal lobes). DifB does not enter the nucleus and co-localizes with a synaptic protein. In males and females, a DifB mutant alters alcohol behavioral sensitivity without an obvious effect on combating infection, whereas a DifA mutant does not affect alcohol sensitivity but compromises the immune response. These data are evidence that the non-nuclear DifB variant contributes to alcohol behavioral sensitivity by a nongenomic mechanism that diverges from the NF-κB transcriptional effects used in the peripheral immune system. Enrichment of DifB in brain regions rich in synapses and biochemical enrichment of DifB in the synaptoneurosome fraction indicates that the protein may act locally at the synapse.

Key words: **alcohol sensitivity; behavior; Drosophila; innate immune system; neuroimmune; synapse**

Significance Statement

NF-κBs are transcription factors used by innate immune signaling pathways to protect against infection. Alcohol abuse also activates these pathways, which contributes to the addictive process and the health consequences associated with alcohol abuse. In the mammalian nervous system, NF-κBs localize to synapses, but it is axiomatic that they effect change by acting in the nucleus. However, for the Drosophila *Dif* gene, immune and neural function segregate into different protein isoforms. Whereas the nuclear isoform (DifA) activates immune genes in response to infection, the CNS isoform acts nongenomically to modulate alcohol sensitivity. Immunohistochemical and biochemical assays localize DifB to synapse-rich regions. Direct synaptic action would provide a novel and rapid way for NF-κB signaling to modulate behavior.

Introduction

Alcohol-use disorder (AUD) is a serious health concern worldwide. In the United States, ~5% of the population have an alcohol-use disorder, and alcohol misuse is the third leading preventable cause of death (Mokdad et al., 2004; Center for Behavioral Health Statistics and Quality, Substance Abuse and Mental Health Services Administration, 2020). Many consequences of alcohol abuse are linked to activation of NF-κB transcription factors, an output of innate immunity Toll-like receptor (TLR) signaling pathways. The role of Toll signaling in activating the innate immune system was discovered in flies and shown to be highly conserved in mammals (Lemaitre et al., 1996; Medzhitov et al., 1997).

Important aspects of alcohol dependence such as compulsive drinking and brain and organ damage are also intertwined with alcohol's effects on innate immune signaling. Chronic alcohol abuse increases expression of TLR signaling components, sensitizing innate neuroimmune pathways to future insults and leading to a state of chronic activation (Crews et al., 2017). Chronic neuroimmune activation promotes neurodegeneration that could contribute

Received Oct. 1, 2021; revised Feb. 2, 2022; accepted Feb. 9, 2022.

Author contributions: T.P.W. and N.S.A. designed research; T.P.W., Z.W., N.P.S., R.G., and L.K.L. performed research; N.S.A. contributed unpublished reagents/analytic tools; T.P.W., Z.W., N.P.S., R.G., and N.S.A. analyzed data; T.P.W. and N.S.A. wrote the first draft of the paper; T.P.W. and N.S.A. edited the paper; N.S.A. wrote the paper.

This work was supported by the National Institute on Alcohol Abuse and Alcoholism Grant 2R01AA018037-06A1 (to N.S.A.). We thank Jane Kirschman for copyediting and other feedback on the manuscript, Adron Harris (University of Texas at Austin) for comments on the manuscript, Steven Wasserman (University of California San Diego) for DifA, DifB, and J4 lines and the anti-DifB antibody, and Dominique Ferrandon (Institut de Biologie Moléculaire et Cellulaire Stasbourge France) for the anti-DifA antibody.

*N.P.S. and R.G. contributed equally to this work.

The authors declare no competing financial interests.

Correspondence should be addressed to Nigel S. Atkinson at nigela@utexas.edu.

https://doi.org/10.1523/JNEUROSCI.1963-21.2022

to the cognitive decline associated with long-term alcohol abuse (Crews et al., 2015). Furthermore, TLR pathway signaling has been causally linked to ethanol consumption and changes in ethanol sensitivity (Erickson et al., 2019).

As in humans, the fly innate immune system is induced by ethanol and also modulates alcohol responses (Troutwine et al., 2016; Crews et al., 2017). Outputs of the adult fly innate immune signaling pathways are the NF-κB transcription factors dorsal-related immunity factor (Dif) and Relish. In adults, Dif is the transcription factor output of the Toll pathway and Relish is the transcription factor output of the IMD pathway (Hoffmann and Reichhart, 2002).

Alternative splicing of Dif transcripts generate mRNAs that encode two different protein isoforms—the so-called DifA and DifB isoforms. The DifA protein is similar to a canonical NF-κB, having a Rel Homology Domain (required for DNA binding, dimerization, and binding to the I-κB homolog Cactus) and a nuclear localization signal (NLS) as well as a transcription activation domain (Ip et al., 1993; Zhou et al., 2015). The DifB variant differs in that the C-terminus lacks the NLS and transactivation domains. In place of these, for the DifB transcript, alternative splicing has substituted a large exon that generates a C-terminal amino acid sequence that is unusual in the NF-κB superfamily (no amino acid sequence similarity other than to that encoded by the dorsal B exon). Zhou et al. (2015) documented DifB expression in the mushroom bodies of the larval brain.

In mammals, a considerable fraction of neural NF-κB protein localizes to the postsynaptic density, and synaptic activity can cause this NF-κB to move to the nucleus, where it modifies gene expression in ways that influence neuronal plasticity (Salles et al., 2014). Because NF-κB is a well-known transcription factor, it is generally held that all the effects of an NF-κB are produced through its action in the nucleus. However, from flies there is strong evidence that synaptic NF-κBs directly modulate neurotransmission (Beramendi et al., 2005; Heckscher et al., 2007; Zhou et al., 2015).

Previously, it was shown that an increase in Toll->Dif signaling induces antimicrobial peptide expression and promotes ethanol resistance while suppression of Toll->Dif signaling increases ethanol sensitivity (Rutschmann et al., 2000; Troutwine et al., 2016). Here, we test the hypothesis that immune responses arise from NF-κB nuclear signaling and that alcohol responses are modulated by non-nuclear, neuronal, NF-κB action. We demonstrate that DifA does not affect alcohol sensitivity but instead activates immune responses. DifB, however, does not activate the immune response and instead acts outside of the nucleus in the nervous system, where it influences alcohol sensitivity. The DifB protein cofractionates with a synaptic protein suggesting that it could directly alter synaptic plasticity. Direct modulation of the synapse by an NF-κB may be important for explaining unusual consequences of neuroimmune dysregulation such as impaired brain function, the exacerbation or cause of mental illnesses, and neurologic complications of Covid-19 disease (Herron et al., 2018; Iadecola et al., 2020).

Materials and Methods

Fly stocks

Flies were raised on corn meal malt extract food [7.6% CH Guenther & Son Pioneer Corn Meal (Walmart Inc.), 7.6% Karo syrup (Walmart Inc.), 1.8% Brewer's yeast (SAF), 0.9% Gelidium agar (MoorAgar Rocklin), 0.1% nipagin (ThermoFisher Scientific Inc.) in 0.5% ethanol, 11.1% #5888 amber malt extract (Austin Homebrew Supply) and 0.5% propionic acid (ThermoFisher Scientific Inc.)]. Solids are weight/volume and liquids are volume/volume. Flies were housed in a 12/12 h light/dark cycle at ~21°C. The DifA and DifB mutant lines and the J4R matched control line was obtained from S. A. Wasserman (University of California San Diego). Behavioral tests were performed on flies that were 5-d-old virgins. Other stocks used are identified by their Bloomington Drosophila Stock Center number: Canton S (wild-type BDSC: 64349), Dif^1 (derived from stock BDSC 36559 by crossing); Tub-Gal4 (BDSC#5138, genotype y^1 w^*; P{w[+mC]=tubP-GAL4} LL7/TM3, Sb^1 Ser^1); deGradFP (BDSC#3842, genotype w^*; P{w[+mC]=UAS-Nslmb-vhhGFP4}3); Cas-9-expressing stock (BDSC#54 591, genotype y^1 M{w[+mC]=nos-Cas9.P}ZH-2A w^*); Cre-recombinase-expressing stock (BDSC#1092, genotype y^1 w[67c23]; sna^{Sco}/CyO, P{w[+mC]=Crew}DH1).

Validation of mutant stocks

Genetic validation

The DifA mutant was validated by amplifying the region spanning the splice site mutation by PCR (catalog #10572-014, PCR Supermix Life Technologies) and sequencing the amplified fragment. The DifB stock was validated by PCR using a forward primer within the REL homology region and a reverse primer within the B exon, to demonstrate loss of the B exon. The parental J4 rescue stock (J4R) was used as the positive control.

Loss-of-expression validation

Adult flies and third instar larvae were dissected and subjected to immunohistochemistry using anti-DifB (Zhou et al., 2015) or anti-DifA (Rutschmann et al., 2000) primary antibodies and anti-Brp (nc82) to confirm that the DifA and DifB mutations eliminated all expression of their respective antigen without affecting expression of the other product. These data also confirm the specificity of the antibodies.

Ethanol sensitivity assay

Ethanol sedation assay

The assay was conducted between 11 A.M. and 4 P.M. to minimize differences that might be attributed to circadian rhythms. The assay was performed as described (Pohl et al., 2013), with minor modifications. Five-day-old age-matched flies, collected as virgins, were tested. On the day of the assay, the flies were loaded into empty food vials at 10 flies per vial. One milliliter of 35% ethanol was pipetted onto a cotton FLUG, cut to 0.5 inches in height and placed at the bottom of the vial. The FLUG is separated from the flies by a Kimwipe. The ethanol vapor concentration in the chamber rises with time and gradually sedates the flies. A computer camera was used to capture the sedation profile of the flies every 30 s. The movement of flies was quantified using a Perl script (sliding-window method) as described by Ramazani et al. (2007) and analyzed using R.

Duration of loss-of-righting reflex assay (also known as recovery from ethanol sedation assay)

The recovery from sedation assay was performed essentially as described (Cowmeadow et al., 2005). Groups of 10 females were placed in plastic vials and exposed to a stream of humidified, saturated ethanol vapor until all flies sedated (typically 15–18 min). Then the ethanol air stream was replaced with a humidified fresh air stream and recovery from sedation was recorded. Flies are considered recovered when they regain postural control. All experiments were performed between 11 and 4 pm. Logrank analysis performed in R.

CRISPR-mediated tagging of Dif A and Dif B isoforms

gRNA and donor plasmids for CRISPR-tagging of DifA and DifB isoforms were designed with assistance from Rainbow Transgenic Flies, Inc. such that the modified genes will express DifA-GFP or DifB-GFP fusion proteins.

gRNA construction

Guide RNAs specific to the genomic region flanking the DifA or DifB STOP codons were identified using the CRISPR Optimal Target finder software (Gratz et al., 2014). Off-target effects were minimized by

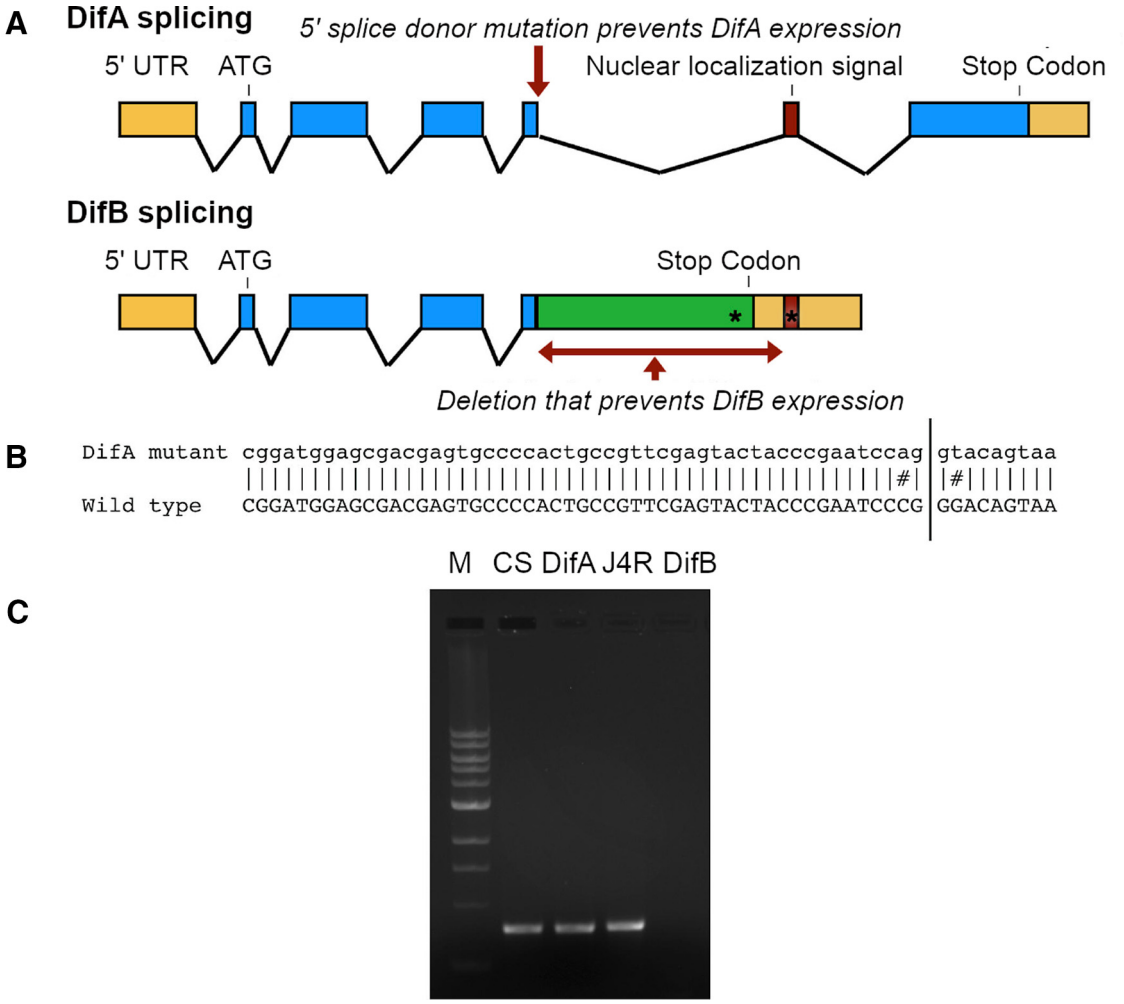

Figure 1. Description of DifA and DifB splice variants and splice variant-specific mutations. ***A***, Splicing pattern of the DifA and DifB splice variants showing the position of a splice site mutation that blocks DifA expression and the deletion that removes the exon required to produce the DifB variant. Asterisks are positions of PCR primers used to validate DifB. The DifA and DifB mutants were validated at the level of genomic DNA. ***B***, Validation of DifA mutant. Mutation of the 5′ splice donor site needed for the production of the DifA variant was confirmed by sequencing of genomic DNA. DifA mutant also carries a silent mutation (C to A transversion) in the last full codon of the 5′ exon. ***C***, Validation of DifB mutant. PCR primers (asterisks in ***A***) were used to confirm the absence of the DifB exon in genomic DNA from the DifB stock. M = DNA markers. The DifB-specific band is present in genomic DNA from the Canton S wild-type (CS), DifA mutant, J4R parental line, but is missing in the DifB mutant.

choosing gRNAs lacking significant homology to any other regions. Double-stranded DNA oligomers encoding the gRNAs were cloned into pCFD3 U3 vectors.

Donor plasmid construction

Two ~1-kb homology arms flanking the DifA stop codon or the DifB stop codon were identified. The upstream homology arm was ligated to a flexible linker 30 n (encodes G_4SG_4S), an 844 n eGFP fragment, and a 121 n SV40 poly A tail-encoding fragment was ligated to a 3′ ~1-kb homology arm and ligated into the vector pleukan-white which provides a floxed miniwhite cassette. The construct will insert eGFP miniwhite cassettes immediately before the DifA or DifB stop codons.

Injection and screening and removal of miniwhite cassette

The cloned gRNA and cloned donor construct were injected into embryos of Cas9-expressing flies y^1 M{w[+mC]=nos-Cas9.P}ZH-2A w^1 (BDSC#54 591). The eclosed founders flies were crossed to w^{1118}; Sco/Cyo;Tm6Tb/MKRS flies and a NightSEA fluorescent illuminator used to identify GFP-positive animals (Model SFA-LFS-GR, NightSEA). Complementation of *w*∗ was used to track modified alleles and a homozygous stock was built. Frequency of successful targeting to the *Dif* locus was 7/330 w^+ animals for Dif A-GFP and 22/350 w^+ animals for Dif B-GFP. The miniwhite cassette was removed by crossing to a Cre-recombinase expressing line (BDSC#1092; genotype y^1 w[67c23]; sna^{Sco}/CyO, P{w[+mC]=Crew}DH1]) and then screening for white-eyed flies. The area flanking the eGFP cassette was PCR amplified sequenced to validate the integrity of the final product.

Infection with *Beauveria bassiana* and survival analysis

B. bassiana (ATCC strain #44860 obtained from American Type Culture Collection) was grown to confluence at 25°C for 14 d on Potato Dextrose Agar. After this period, microscopic inspection indicated substantial sporulation. The spores were eluted from a Petri dish with 10 ml of filter sterilized 0.01% Triton X-100 and transferred into 1.5-ml Microfuge tubes. All fly strains (3-5 d old) to be compared were infected with the same eluant immediately after its collection. To infect, a minuten pin (catalog #26002-20, FST Group), dipped into the spore suspension was used to pinprick the fly in the thorax near the haltere. Flies that died within the first day were excluded from analysis (usually <1%). Controls included flies that were pinpricked with a clean (spore-free needle) and flies that were not pinpricked at all. Males and females were assayed separately. Following pinprick or control manipulation, the survival of flies was monitored in vials containing fly food absent the antifungal agents, propionic acid and nipagin. Each vial contained ~10 flies. For at least 10 d, dead flies were counted every 24 h, and living flies were transferred to a new vial containing fresh food. These protocols were derived from multiple publications (Vandenberg, 1996; Rutschmann et al., 2000; Kamp and Bidochka, 2002;

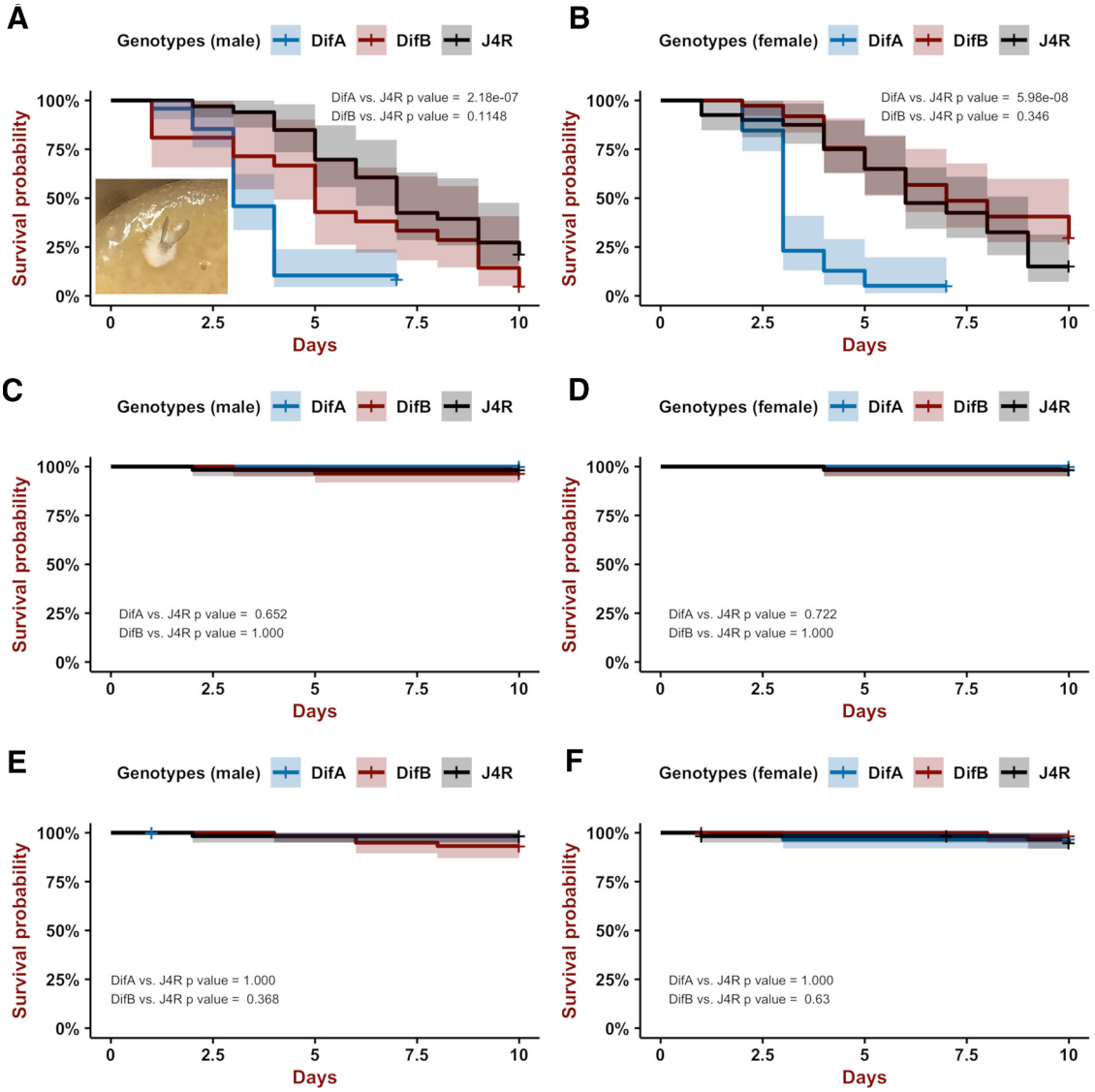

Figure 2. Kaplan–Meier plots showing that loss of DifA has a large effect on mortality after *B. bassiana* infection. Shown is probability of survival versus days. Blue is DifA mutant, red is DifB mutant, and black is a J4R genetically matched control. Bonferroni-corrected Logrank statistics are used to determine significance. Vertical tic lines on the plot are censored observations. Shading is the 95% confidence interval. ***A***, ***B*** are males and females, respectively. ***A***, Only DifA mutants (blue) die more rapidly than the J4R line (wild-type control for DifA and DifB) after a stabbing-mediated infection (DifA $n = 48$; DifB $n = 21$; J4R $n = 33$; DifA vs J4 $p = 2.181838 \times 10^{-7}$, Chisq = 28.2 on 1 df; DifB vs J4 $p = 0.11474676$, Chisq = 3.6 on 1 df). Inset shows a DifA corpse ~2 d after death with fungus emerging from body. Growth of fungus was not checked for all corpses. ***B***, In females, DifA mutants are extremely sensitive to *B. bassiana* infection whereas DifB mutants do not show increased sensitivity to *B. bassiana* infection compared with the J4R control (DifA $n = 39$; DifB $n = 37$; J4R $n = 40$; Logrank statistics; DifA vs J4 $p = 5.980564 \times 10^{-8}$, Chisq = 30.7 on 1 df; DifB vs J4 $p = 0.3457584$, Chisq = 1.9 on 1 df). ***C***, ***D*** are males and females, respectively. Neither have been stabbed or infected with *B. bassiana*. DifA and DifB mutations do not affect longevity over a 10-d period when compared with the J4R line. ***C***, Probability of survival versus days for male flies (DifA $n = 58$; DifB $n = 57$; J4R $n = 60$; DifA vs J4 $p = 0.6510258$, Chisq = 1 on 1 df; DifB vs J4 $p = 1.000$). ***D***, Probability of survival versus days for female flies (DifA $n = 50$; DifB $n = 58$; J4R $n = 60$; DifA vs J4 $p = 0.7226208$, Chisq = 0.8 on 1 df; DifB vs J4 $p = 1.000$, Chisq = 0 on 1 df). ***E***, ***F*** are males and females, respectively, stabbed with a needle that has not been coated with *B. bassiana* spores. A single stab wound in the lower thorax has no effect on longevity over a 10-d period. ***E***, For males DifA $n = 60$; DifB $n = 59$; J4R $n = 58$; DifA versus J4 $p = 1.000$, Chisq = 0 on 1 df; DifB versus J4 $p = 0.3678934$, Chisq = 1.8 on 1 df. ***F***, For females DifA $n = 59$; DifB $n = 57$; J4R $n = 58$; DifA versus J4 $p = 1.000$, Chisq = 0.2 on 1 df; DifB versus J4 $p = 0.6300112$, Chisq = 1 on 1 df.

Khalil et al., 2015). Logrank statistical analysis of survival was performed in R using the packages "survival" and "survminer."

Capillary Feeder assay (CAFE)-alcohol preference/consumption assay

To measure differences in alcohol consumption and preference in flies, we used the CAFE essentially as previously described (Park et al., 2018). Male flies were collected at 1 d of age and stored in groups of 10 until they were 5 d old. Female flies were collected at eclosion (virgin) and aged in groups of 10 until 5 d of age. Each test vial contained two 5-μl microcapillary tubes (catalog #21-180-11, Drummond Scientific Company). One microcapillary contained liquid food and the other microcapillary contained liquid food plus 5% ethanol. Liquid food was 5% yeast extract and 5% sucrose. The microcapillaries were passed through the cotton flug at the top of the vials. Each vial also contained ~1 ml of standard fly food at the bottom of the vial. Vials were incubated for 3 d at 25°C with high humidity and 12/12 h light/dark illumination. Data were collected at the end of the light period. Control vials containing the microcapillaries but no flies were used to account for evaporation.

Confocal immunohistochemistry

Antibody staining of adult brain, larval brains, and larval fat body were performed as follows. The brains of 4- to 5-d-old adult flies or third

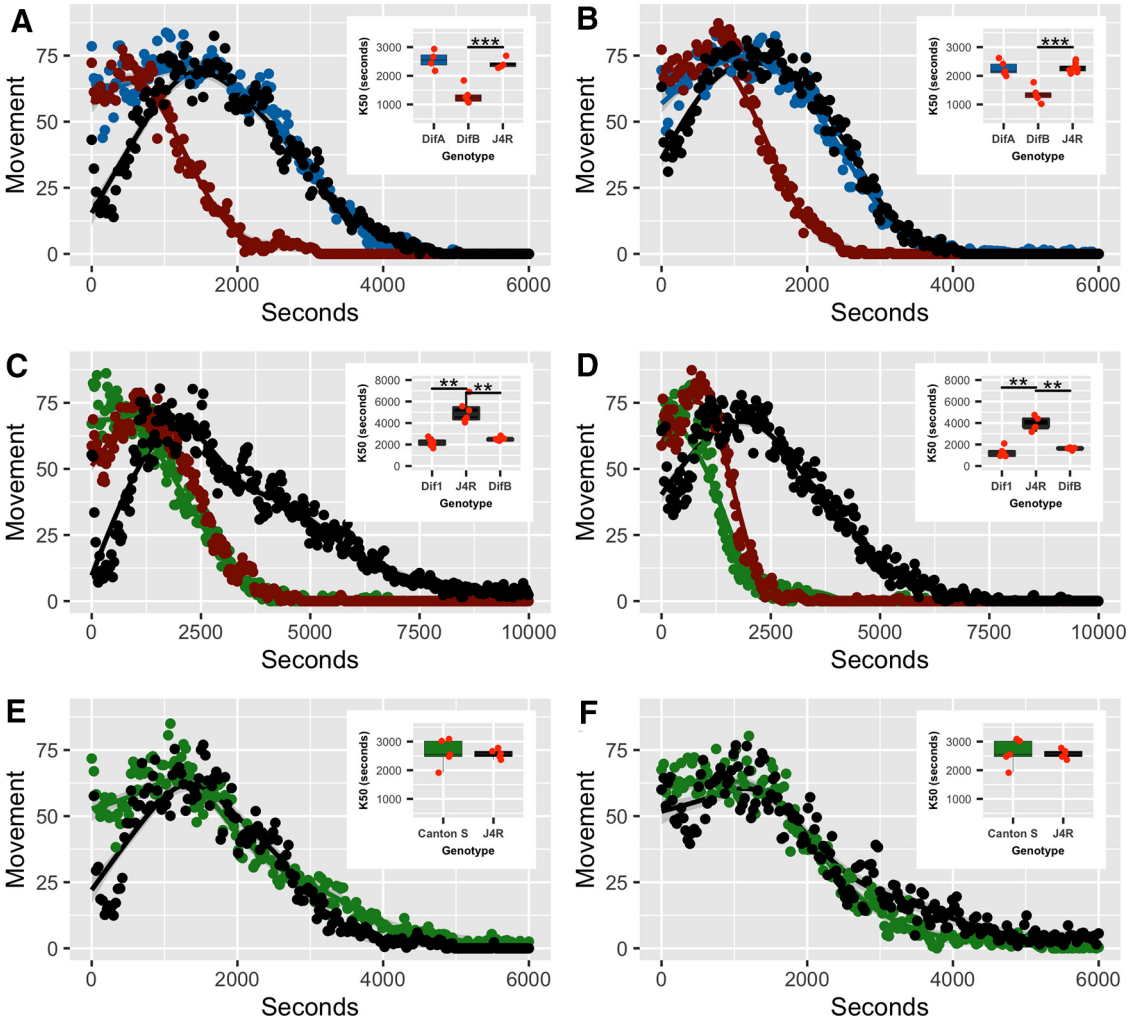

Figure 3. Loss of the DifB variant increases sensitivity to sedation with vapor from a 35% ethanol solution. Points are average movement at each time point and line is best fit. Inset shows the t1/2 for each genotype (time to sedation of 50% of the sample). In males (***A***) and females (***B***), the DifB mutation, but not the DifA mutation, increases the sensitivity to sedation with ethanol vapor compared with the J4R parental control line. Male and female data approximate normality and equal variance (Shapiro test and *F* test > 0.05, respectively). For male KD50, ANOVA df = 2, *F* value = 27.03, and $p = 9.27 \times 10^{-5}$. Dunnett *post hoc* test for DifA versus J4R $p = 0.721823$ and DifB versus J4R $p = 0.000299$. $N = 5$–7. For female KD50, ANOVA df = 2, *F* value = 27.66 and $p = 1.37 \times 10^{-5}$. Dunnett *post hoc* test for DifA versus J4R $p = 0.985$ and DifB versus J4R $p = 1.63 \times 10^{-5}$. $N = 4$–5. In males (***C***) and females (***D***), the DifB mutation appears to completely account for the magnitude of increased ethanol sensitivity caused by the *Dif* ^{1} mutation, which maps to a region shared by the DifA and DifB variants. Here, male and female data approximate normality and but have unequal variance (Shapiro test > 0.05 and *F* test are < 0.05, respectively), and so we used the Kruskal–Wallis rank-sum test in place of ANOVA. Bonferroni corrected Mann–Whitney *post hoc* tests were used to determine *p* values relative to J4R line. For male KD50, Kruskal–Wallis rank-sum test, df = 2, Chisq = 12.784, and $p = 0.001675$. *Dif* ^{1} versus J4R $p = 0.004329004$, DifB versus J4R $p = 0.004329004$. $N = 6$. For female KD50, Kruskal–Wallis rank-sum test df = 2, Chisq = 10.5 and $p = 0.005248$. *Dif* ^{1} versus J4R $p = 0.016$. DifB versus J4R $p = 0.016$. $N = 5$. ***E***, ***F*** show that male and female Canton S and J4R have similar sedation profiles and indistinguishable KD50 values. ***E***, Male data approximate normality but have unequal variance (Shapiro test and *F* test, respectively). Therefore, we used the Welch test for this comparison $p = 0.8739$. $N = 5$. ***F***, Female data approximate normality and equal variance (Shapiro test and *F* test, respectively); therefore, we used a Student's *t* test for this comparison $p = 0.5213$, $N = 5$.

instar larvae were dissected in 1× PBS and fixed in freshly prepared 4% paraformaldehyde in PBHS (PBS plus 1 M NaCl) for 20 min at room temperature. All subsequent procedures were performed at room temperature, except for antibody incubations. Tissues were washed three times in 1× PBHS plus 0.5% Triton X-100 for 15 min each and then washed three times in 0.1 M Tris-HCl/0.3 M NaCl (pH 7.4) containing 0.5% Triton X-100 (TNT) for 15 min each. Blocking was performed in TNT solution containing 4% normal goat serum (blocking buffer catalog #005-000-001, Jackson ImmunoResearch) for 1.5 h. The primary antibody was applied in blocking solution and incubated ~36 h at 4°C [rabbit anti-DifA: 1:2000 dilution; gift from Dominique Ferrandon, French National Center for Scientific Research (CNRS), France; and rabbit anti-DifB 1:2000 dilution, gift from S. A. Wasserman, University of California San Diego, CA; and mouse anti-Brp 1:20 dilution, ID #AB_2314866, Developmental Studies Hybridoma Bank and rabbit anti-GFP 1:1000, catalog #A11122, ThermoFisher Scientific/Invitrogen]. Brains were rinsed six times for 15 min each and five times for 30 min each in TNT. Brains were incubated ~36 h at 4°C in secondary antibody diluted in blocking solution and [Alexa Fluor 488 goat anti-rabbit: 1:400; catalog #111-545-144 (Jackson ImmunoResearch); Alexa Fluor 635 goat anti-mouse: 1:200, catalog #A-31575 ThermoFisher Scientific/Invitrogen)]. Tissues were washed six times for 15 min each. Fluorescently labeled tissues were mounted in DAPI Fluoromount-G (catalog #0100-20, SouthernBiotech). For double-staining experiments, following a single round of blocking, antibody stainings were performed sequentially. Tissues were imaged with a Zeiss 710 confocal microscope and captured using the Zen Black software (Carl Zeiss Microscopy, LLC) except for Figure 13, which was imaged on a Leica SP8X microscope using a 93× glycerol objective with motorized correction collar and processed using Leica's LIGHTING adaptive deconvolution algorithm. Z stacks were composed of 1-µm optical sections.

Colocalization analysis

Colocalization analysis was performed using the Zen-Blue image analysis colocalization software (Carl Zeiss Microscopy, LLC). The brains of wild-type Canton S flies were stained using anti-DifB primary antibody and Alexa Fluor 488 secondary antibody and mounted in DAPI-containing fluoromount-G mounting medium. Thresholds were set using Canton S brains that were stained with only the DifB antibody and Alexa Fluor 488 secondary antibody in Fluoromount-G without DAPI (catalog #0100-01, SouthernBiotech) or with only DAPI Fluoromount-G according to the Zen-Blue instructions. Laser gain and magnification were not changed once the thresholds were set. The Zen-Blue image analysis colocalization function was then used to determine the Pearson's correlation coefficients for each image in the Z stack.

Synaptoneurosome and nuclei fraction preparation

The synaptoneurosome preparation protocol was a substantial modification of a previously reported protocol (Depner et al., 2014), while the protocol for enriching for the nuclei fraction was based on different sources (Shaffer et al., 1994; Yin and Lin, 2014). Homogenate buffer: 0.32 M sucrose, 4 mM HEPES, 1× Protease Inhibitor Cocktail. Buffer A: 60 mM KCl, 15 mM NaCl, 1 mM EDTA (pH 8.0), 0.1 mM EGTA, 15 mM HEPES (pH 7.4), 0.5 mM DTT, 0.1% Triton X-100, 1× Protease Inhibitor Cocktail. Buffer AS: 60 mM KCl, 15 mM NaCl, 1 mM EDTA (pH 8.0), 0.1 mM EGTA, 15 mM HEPES (pH 7.4), 0.3 M sucrose, 1× cOmplete, EDTA-free Protease Inhibitor Cocktail (catalog #11873580001, Millipore Sigma/Roche Diagnostics GmbH). Prechill homogenization buffer, buffer A, buffer AS on ice.

Preparation of homogenate

Prechill 15-ml tubes, sieves, spatula, funnels, mortar, and pestle in liquid nitrogen. Ten to 25 ml of adult flies in a 50-ml tube were frozen with liquid nitrogen. The flies were vortexed for 1 min to decapitate. Heads were filtered with shaking through with 710-μm aperture sieve and collected in a sieve with a 400-μm aperture. Fly heads were ground for 5–10 min to a fine powder in a prechilled mortar and transferred into a 15-ml tube on ice; 7.5-ml ice-cold homogenization buffer was added and the material was suspended in the buffer with a 10 ml pipette tip. Mixture was homogenized 10–20 strokes at 900 rpm in a 10-ml glass and Teflon homogenizer and moved to a fresh tube. An additional 5 ml of homogenization buffer was added to the original tube and homogenized (5 strokes/900 rpm). Both samples were pooled and mixed by inversion. Large fragments were removed by pushing the homogenate through a 75-μm filter and then a 25-μm filter using a large syringe. An aliquot of 150 μl of homogenate was held back for a protein assay (100 μl) and for slot blotting (50 μl).

Differential centrifugation

The following was on ice or at 4°C. Homogenate was transferred into a 16-ml centrifuge tube and spun at 1000 × *g* for 10 min in a SS34 rotor. Resulting P1 pellet was used for preparation of crude nuclear fraction (below). The supernatant was centrifuged at 15,000 × *g* for 30 min in a SS34 rotor. Supernatant was gently removed to leave the P2 pellet. The cortical part (soft) of the P2 pellet was enriched in synaptoneurosomes. The P2 pellet was gently shaken and the cortical synaptosome region slid away from the denser center of the pellet (presumed to be mitochondria). The cortical region of P2 was resuspended using a 200 μl or larger pipettor.

Crude nuclei fraction

The following was performed on ice or as close to 0°C as possible. Added 5-ml buffer A to the P1 pellet and homogenized for 10 strokes at 900 rpm in a glass and Teflon homogenizer. The homogenate was gently layered on top of 2 ml buffer AS in a 16-ml centrifuge tube using a 1-ml pipette. The nuclei homogenate floated on top of buffer AS and then centrifuged at 1500 × *g* for 5 min in a SS34 rotor. Removed supernatant and resuspended pellet enriched in nuclei in 1 ml of homogenate buffer.

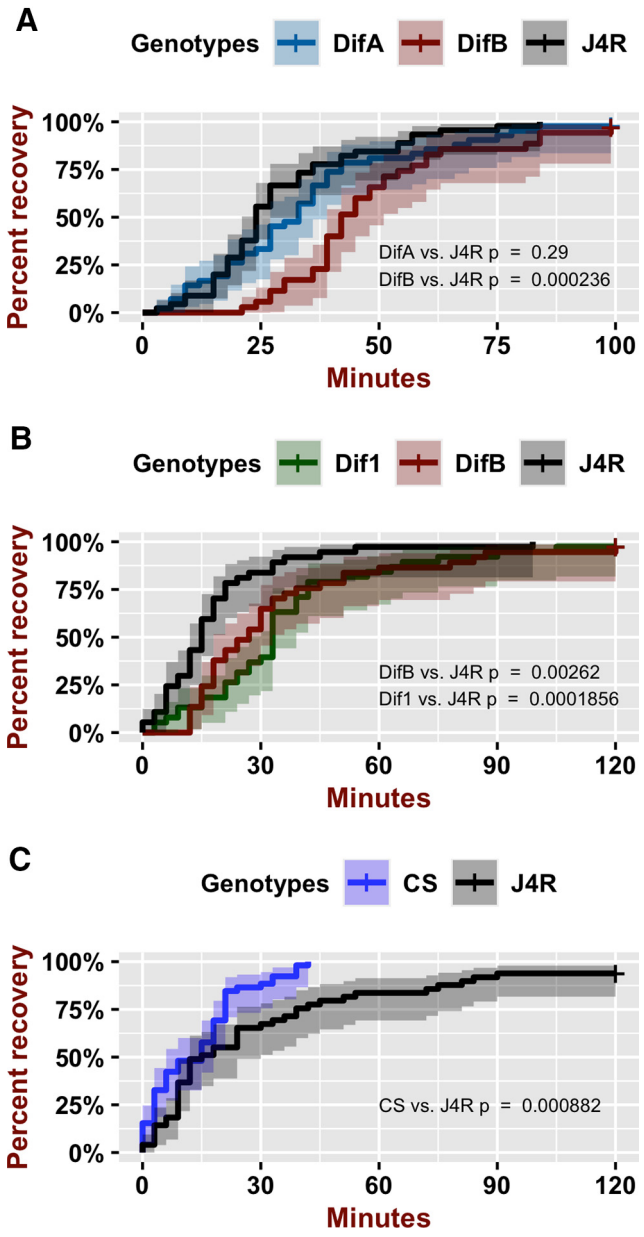

Figure 4. Loss of the DifB variant increases ethanol sensitivity in a recovery-from-sedation assay. Kaplan–Meier plots of recovery from ethanol sedation. Females were sedated with vapor generated from a 100% ethanol solution, switched to an ethanol-free air stream at minutes = 0, and then monitored for recovery from sedation. Bonferroni-corrected Logrank statistics are used to determine significance. Vertical tic lines on the plot are censored observations. Shading is the 95% confidence interval. ***A***, Comparison of the recovery profile of DifA mutant, DifB mutant, and the J4R-positive control line. J4R is genetically matched to DifA and DifB lines, except that it is wild type for both splice variants. The DifB mutation increases ethanol sensitivity but the DifA mutation does not ($N = 4$; DifA vs J4 Chisq = 2.1 on 1 df $p = 0.2902514$; DifB vs J4 Chisq = 14.8 on 1 df $p = 0.000236671$). ***B***, Comparison of recovery profiles for the *Dif* ^{1} mutant, the DifB mutant, and J4R-positive control line. Loss of DifB alone completely accounts for the increase in ethanol sensitivity caused by the *Dif* ^{1} functional null allele ($N = 4$; DifB vs J4 Chisq = 10.3 on 1 df $p = 0.002625412$; Dif1 vs J4 Chisq = 15.3 on 1 df $p = 1.8561352 \times 10^{-4}$). ***C***, Comparison of the J4R-positive control to a Canton S wild-type stock. Canton S is slightly more ethanol resistant than the J4R line ($N = 6$; CS vs J4 Chisq = 11.1 on 1 df $p = 0.000882288$).

Slot blot procedure

The nuclear and synaptosome protein fractions, were probed for the presence of DifB using anti-DifB antibody. The integrity of the nuclear and synaptosome fractions was established by probing for marker proteins: histone H3 for nuclear fraction and Brp for the synaptoneurosome

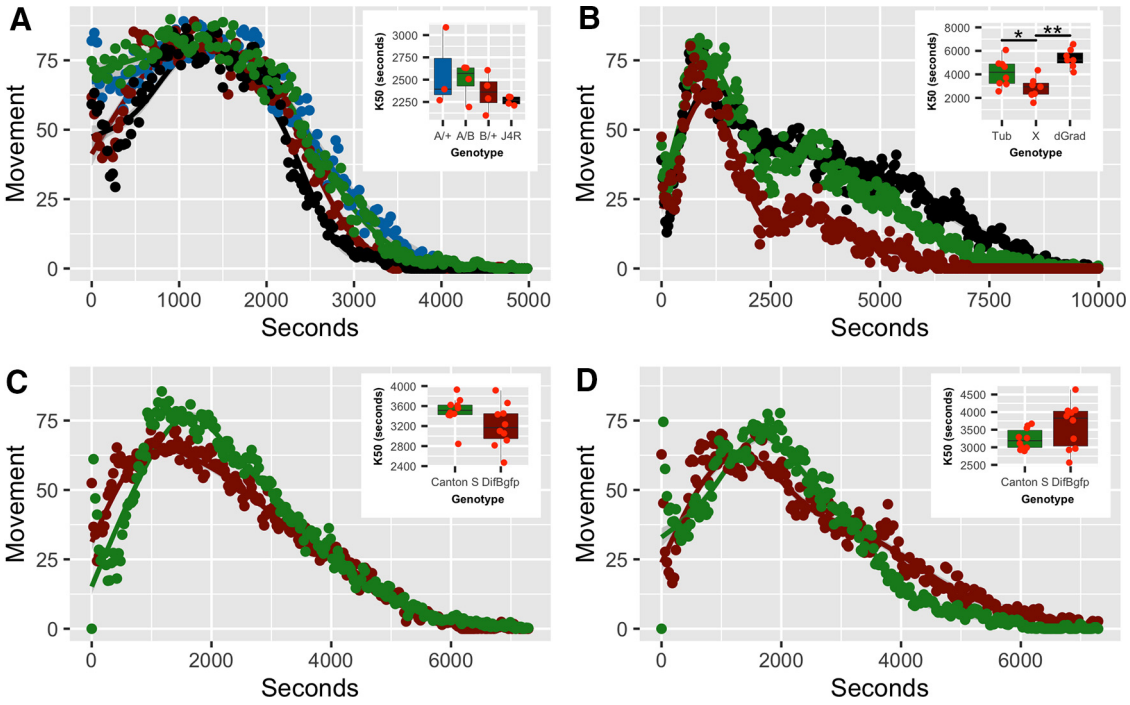

Figure 5. The DifB mutation is recessive, deGradFP knock-down of DifB produces ethanol sensitivity, and GFP tagging of DifB does not affect ethanol sensitivity. Points are average movement at each time point and line is best fit. Inset shows the t1/2 value for each genotype (time to sedation of 50% of the sample). ***A***, The DifA and DifB mutant alleles are recessive. Comparison of heterozygotes shows that all (DifA/+, DifB/+, DifA/DifB) are indistinguishable from the J4R homozygous control [because data does not have equal variance (*F* test) but approximates a normal distribution (Shapiro test), we used ANOVA not assuming equal variance $F = 1.667$, df = 3, $p = 0.2966$; $N = 3–4$)]. ***B***, deGradFP knock-down of DifB (Caussinus et al., 2012) produces ethanol sensitivity. Tubulin Gal4 Driver (Tub) and UAS-Nslmb-vhhGFP (referred to as dGrad in the figure) transgene were crossed to produce Tubulin Gal4 Driver/UAS-Nslmb-vhhGFP transheterozygous males (X in figure). Data have equal variance (*F* test) and approximates a normal distribution (Shapiro test). ANOVA $p = 0.000555$ with df = 2 and $F = 11.41$. Dunnett *post hoc* comparison TubxdGrad versus dGrad $p = 0.000253$ and TubxdGrad versus Tub $p = 0.036037$ ($N = 7–8$). ***C***, ***D***, CRISPR-mediated tagging of the DifB isoform with eGFP does not alter ethanol sensitivity. $N = 10$ for both genotypes and sexes. ***C*** are males [data have equal variance (*F* test) and approximate a normal distribution (Shapiro test); Student's *t* test equal variance $p = 0.08065911$]. ***D*** are females [data approximate a normal distribution (Shapiro test) but do not have equal variance (*F* test); therefore, we used a Welch test $p = 0.11998270$].

fraction. From each sample, 200 ng of total protein was used to probe for Brp, H3, or DifB. Protein concentration determined using Bio-Rad Protein Assay (catalog #5000001, Bio-Rad). Immobilon-P PVDF membrane (catalog #IPVH00010, Millipore Sigma) was equilibrated for 15 s in 100% methanol, soaked in deionized water for 2 min, and incubated for 1 h in PBST (PBS + 0.05% Tween 20). Whatman-filter paper Grade 4 (catalog #1004-917, GE Healthcare UK Limited) was soaked in PBST and placed on the slot blot apparatus (MinifoldII Slot-blotter catalog #SRC 072/0, Schleicher & Schuell). The equilibrated PVDF membrane was placed on top of the filter paper and clamped into the apparatus according to the manufacturer's instructions. Ten-microliter samples diluted to contain 200 ng total protein were taken from the total head homogenate, the nuclear fraction (P2 fraction) and the synaptosome fraction (P3 fraction) and pipetted into the individual slots of the slot blot apparatus. The samples were fixed onto the membranes using vacuum suction. The membranes were then blocked in PBST + 2% nonfat milk for 2 h, and incubated with the primary antibody diluted in blocking solution overnight at 4°C. After three 5-min washes with PBST, they were incubated in secondary antibody diluted in blocking solution for 30 min. The membranes were washed three times for 10 min each in PBST solution and developed using the Clarity Western ECL chemiluminescent kit (catalog #1705060, Bio-Rad) and CL-Xposure X-ray film (catalog #34089, Thermo Scientific) and an automatic film processor (Kodak X-OMAT 1000A Film Processor Model 1000A). Exposure time of the film was adjusted to avoid saturation. Dilution used for each primary antibody was 1:20,000 for rabbit anti-DifB; 1:100 for mouse anti-Brp (nc82); and 1:10,000 for rabbit anti-acetyl-H3 (anti-acetyl-histone H3 antibody catalog #06-599, Millipore Sigma). Anti-DifA, anti-DifB, and anti-Brp are described under confocal immunohistochemistry. Dilution used for each secondary antibody was 1:10,000 for goat anti-rabbit HRP and 1:10,000 for rabbit anti-mouse HRP (catalog #ab6721 and catalog #ab6728, respectively; both are from Abcam). Bands on the x-ray films were quantified for their intensity, corresponding to protein abundance using ImageJ (https://imagej.nih.gov/ij/). Specific activity for each protein is expressed normalized to the summed specific activity of both fractions.

Knock-down of DifB-GFP by deGradFP

Five-day-old Tub-GAL4 x deGradFP flies were behaviorally tested as described above. deGradFP, also called Nslmb-vhhGFP4, targets GFP and GFP-fusion proteins (DifB-GFP) for degradation (Caussinus et al., 2012). Knock-down of the GFP-tagged DifB was visually confirmed using confocal microscopy to monitor the loss of native GFP fluorescence (no paraformaldehyde fixation) in Tub-GAL4-driven UAS-Nslmb-vhhGFP4 transheterozygotes in comparison to control flies containing only Tub-GAL4 and UAS-Nslmb-vhhGFP4. Dissected brains were mounted in Fluoromount G containing DAPI medium.

SCope analysis of gene expression

SCope is a visualization tool (Davie et al., 2018) that we used to examine single cell transcriptomic data by Croset and colleagues (CentralBrain_10k dataset; Croset et al., 2018). The software permits the entry of gene names (not splice variants). *Dif* was entered for the red channel and *elaV* (neural-specific gene) for the green channel. Sensitivity sliders were adjusted to present three colors: red for *Dif*, green for *elaV*, and yellow for overlap between the two (otherwise both *Dif* and elaV transcript abundance could generate similar shades of gray to confuse the interpretation of location). The identification map of clusters is from Croset et al. (2018). The website address for Scope is https://scope.aertslab.org/.

Experimental design and statistical analyses

Molecular biology was used to validate that mutants contained the correct genetic lesions and then the mutants were used to validate the

specificity of isoform-specific antibodies. As much as is possible all conclusions are based on two independent measures. We decided that the protein expression pattern of each isoform should be determined using antibodies against the native proteins and confirmed using anti-GFP staining to detect the expression of GFP-tagged DifA and DifB isoforms. The GFP-tagged isoforms had been created using CRISPR to insert an eGFP coding region immediately before the stop codon of the DifA and DifB coding regions. The DifA and DifB CRISPR modifications were done in different animals so that the isoforms could be distinguished. We asked whether the splice variant mutations affected the immune response because this is the function historically associated with NF-κB proteins and the *Dif* gene in particular. With respect to sensitivity of different mutants to *B. bassiana* infection (produced by pricking the animals with a pathogen-dipped needle), we also documented whether the mutations alone shortened life and whether needle puncture without pathogen shortened life (they did not). We tested for effects on ethanol responses because the *Dif* gene and innate immune signaling have both previously been associated with ethanol responses. To confirm that the absence of DifB protein was by itself responsible for increased ethanol sensitivity we asked whether a DifB mutation reproduced the ethanol sensitivity associated with a presumptive null Dif^1 allele (it did) and whether the loss of DifA protein influenced ethanol sensitivity (it did not). For this purpose, we used a sedation assay and a recovery from sedation assay (also known as duration of loss-of-righting reflex assay). In order to rule out the chance that the DifB phenotype was caused by unknown differences in genetic background we also tested an independent method of knocking down DifB (so-called inducible deGradFP system). The hypothesis that DifB localizes to synaptic regions is based on two independent measures. The first is confocal imaging of brain structures stained with anti-DifB antibody. Staining was localized to the neuropil. In insects, neuropil is mostly devoid of nuclei but rich in synapses. The second measure was a biochemical method in which a previously published synaptoneurosome preparation was first optimized to produce good separation of a synaptoneurosome protein and a nuclear protein and then used to determine which compartment was enriched for DifB protein. To evaluate the correlation or anticorrelation between the DifB isoform and nuclei we used three measures. The first measure was a visual inspection of all confocal sections of an organ. The second was an unsupervised software method that generates a Pearson's correlation coefficient of the intersection between nuclei and DifB. The third measure was the biochemical fractionation method in which a nuclear fraction and a synaptoneurosome fraction was produced. We asked whether DifB co-purified with a nuclear protein or away from a nuclear protein. It co-purified away from the nuclear protein.

Biological replicates, statistical tests, critical values, and outcomes are reported in individual figure legends. R was used for all statistical analyses except Pearson's correlation coefficient. Data analyzed using parametric tests first passed tests for normality (Shapiro test, $p > 0.05$). An F test ($p > 0.05$) was then used to determine whether the datasets had approximately equal variance. A two-tailed Student's t test was used if only two items were to be compared and if the data were normally distributed and had equal variance. The Welch test was used for data with unequal variance. One-way ANOVA followed by Dunnett *post hoc* test was used when more than two datasets were to be compared and the data approximated a normal distribution. If such data did not have equal variance, then one-way ANOVA with unequal variance was used. Data that were not normally distributed were analyzed using the Mann–Whitney test for pairwise comparison and Kruskal–Wallis test when more than two datasets were compared. Time-to-event analysis (death following infection or recovery-from-ethanol sedation) were evaluated using the nonparametric time-to-event Logrank test. All data were Bonferroni multiple comparison corrected when appropriate. Results were considered significant when $p < 0.05$. Zen-Blue calculated Pearson's correlation coefficient was used to evaluate the correlation between DifB and nuclei in confocal image stacks.

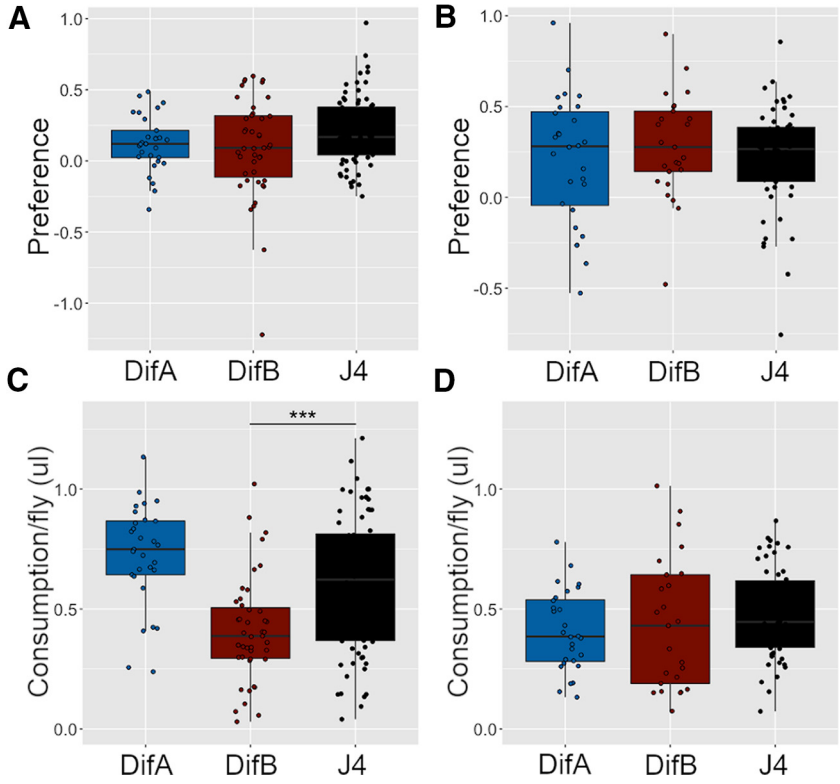

Figure 6. Neither DifA nor DifB mutants affect ethanol preference as measured in the CAFE assay. DifA mutant, DifB mutant, and the control J4R lines show similar ethanol preference in (***A***) females and (***B***) males [data were not normally distributed (Shapiro test) and so we used a Kruskal–Wallis rank-sum test $\chi = 3.349$, df = 2, $p = 0.1873993$ and $\chi = 0.7211$, df = 2, $p = 0.6972941$, respectively; $N = 28–72$]. ***C***, ***D*** are total fluid consumption. ***C***, The DifB mutation reduces total fluid consumption in females [data approximate a normal distribution (Shapiro test) and have equal variance (F test), so we used one-way ANOVA $F = 14.68$, df = 2, $p = 1.62 \times 10^{-6}$ with Dunnett *post hoc* test, ***$p = 0.00019$]. Neither the DifA nor DifB mutants alter total fluid consumption in males [data approximated a normal distribution (Shapiro test) but had unequal variance and so we used one-way ANOVA, not assuming equal variances $F = 1.5443$, df = 2, $p = 0.2233$]. Same flies in ***A***, ***C*** and in ***B***, ***D***.

Results

Validation of mutants and control

The *Dif* gene produces two protein isoforms by alternative mRNA splicing (Zhou et al., 2015). The so-called DifA variant encodes a protein of 667 aa that begins with a Rel domain, includes a NLS and a transactivation domain. The DifB variant encodes a longer 987-aa protein that also begins with a Rel domain but replaces the NLS and transactivation domains with a sequence of 628 aa (Fig. 1*A*). The terminus, encoded by a single exon, has not yet been associated with any orthologous sequences in mammals. Zhou et al. (2015) built a DifA mutant allele and a DifB mutant allele that specifically eliminated expression of one or the other protein isoforms. These mutants and a DifA+, DifB+ genetically matched control called J4rescue (later referred to as J4R) provide an ideal set of tools for determining the function of the DifA and DifB NF-κB isoforms. We validated the DifA-specific and DifB-

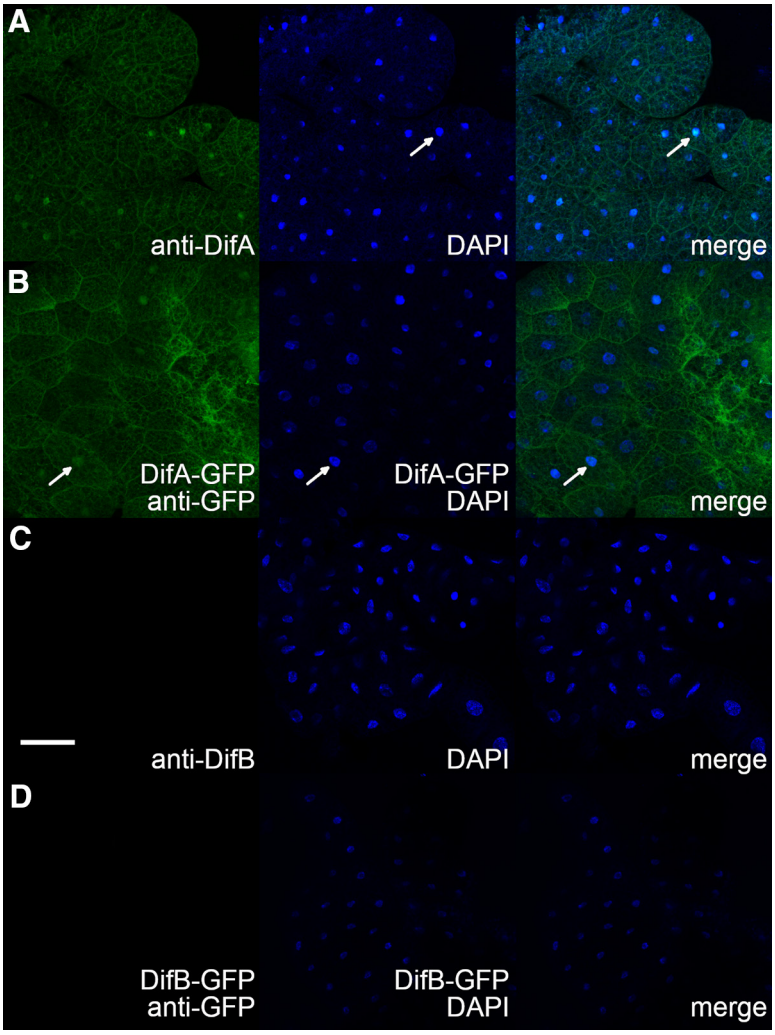

Figure 7. DifA but not DifB is expressed in the fat body. Left column is antibody-stained larval fat body, middle panel is DAPI-stained larval fat body, and the right column is the merged image. Row ***A***, Dissected larval fat bodies co-stained with anti-DifA antibody and DAPI show that DifA and nuclei can colocalize (Canton S wild-type stock). Row ***B***, CRISPR was used to tag the DifA splice variant with an inframe eGFP cassette. Immunohistochemical staining with anti-GFP shows that the tagged DifA protein also colocalizes with the nucleus. Also note that both anti-DifA and anti-GFP staining of DifA-GFP show localization to the cell membrane. Row ***C***, Anti-DifB antibody does not stain an antigen in the fat body (Canton S wild-type stock). Row ***D***, CRISPR was used to tag the DifB splice variant with an inframe eGFP cassette. Immunohistochemical staining with anti-GFP antibody confirms that DifB protein expression is not detectable. Scale bar: 100 μm.

specific mutations and the J4R line at the genomic level by genomic PCR and DNA sequencing (Fig. 1*B*,*C*).

DifA, but not DifB, is critical for immune function

Invertebrates have an innate immune system that has substantial orthology with the mammalian innate immune system (Hoffmann, 2003). *Drosophila* adults have two NF-κB genes that mediate their innate immune response. The *Dif* gene encodes an NF-κB that activates the immune response against fungi and Gram-positive bacteria, whereas the *Rel* gene encodes an NF-κB that mediates the response to Gram-negative bacteria and some Gram-positive bacteria (Hedengren-Olcott et al., 2004).

To determine which Dif isoforms activate the immune system in response to infection, we compared the capacity of the DifA mutant, the DifB mutant, and the J4R control line to survive infection with *B. bassiana*, an entomopathogenic fungus that causes white muscadine disease in insects (Soumia et al., 2021). Flies were infected by stabbing with a minuten pin dipped in a suspension of *B. bassiana* spores and scored for mortality daily for at least 10 d. All strains and both sexes showed increased mortality after stabbing inoculation (Fig. 2*A*,*B*).

However, the DifA mutant showed a much higher rate of death after infection than did the DifB mutant or the J4R line. After infection, the rate of death of the DifB mutant and J4R line were statistically indistinguishable (albeit we have sometimes observed that the DifB mutant displays a statistically insignificant increase in sensitivity compared with the J4R line; Fig. 2*A*). The DifA and DifB mutations do not reduce viability in the absence of infection (Fig. 2*C*,*D*), and a mock stabbing inoculation (minuten pin stabbing absent *B. bassiana* spores) did not reduce fly viability over a 10-d period for either of the mutant lines (Fig. 2*E*,*F*) compared with the J4R control. These data indicate that the DifA NF-κB variant, but not the DifB NF-κB variant, plays a major role in immune protection against infection.

Loss of DifB, but not of DifA, increases ethanol sensitivity

Previously, we had reported that the Dif^1 allele, a mutation in an exon common to both DifA and DifB variants, greatly increased the sensitivity of flies to ethanol vapor sedation (Troutwine et al., 2016). Figure 3*A*,*B* shows that it is the loss of DifB activity but not the loss of DifA activity that increases ethanol-sedation sensitivity. A camera was used to monitor movement of flies in vials as they are exposed to the vapor from a 35% ethanol solution (Pohl et al., 2013). The concentration of ethanol vapor climbs in the vial over time. Initially, the low concentrations of vapor act as a stimulant and the flies move more. When the concentration is sufficiently high, the flies sedate. Sedation times vary daily, apparently because of changes in rate of ethanol evaporation, and therefore all flies to be compared are tested at the same time (Pohl et al., 2013). The DifB mutants show increased locomotor activity and sedation at earlier time points than either the J4R control or the DifA mutant. The DifA mutant and J4R control line are indistinguishable in this assay. The DifB mutant, but not the DifA mutant, also causes an increase in ethanol sensitivity in a duration of ethanol loss-of-righting reflex assay (Fig. 4*A*). Furthermore, we observed that the increase in ethanol sensitivity caused by the Dif^1 allele can be completely accounted for by the loss of DifB expression in both the sedation and duration of loss-of-righting reflex assay (Figs. 3*C*,*D*, 4*B*). In addition, deGradFP knock-down (Caussinus et al., 2012) of an eGFP-tagged DifB splice variant also resulted in increased ethanol sensitivity (Fig. 5*B*). Finally, the J4R line, which serves as our primary control line, and a wild-type Canton S line showed indistinguishable ethanol sensitivity in the sedation assay (Fig. 3*E*,*F*). However, J4R did

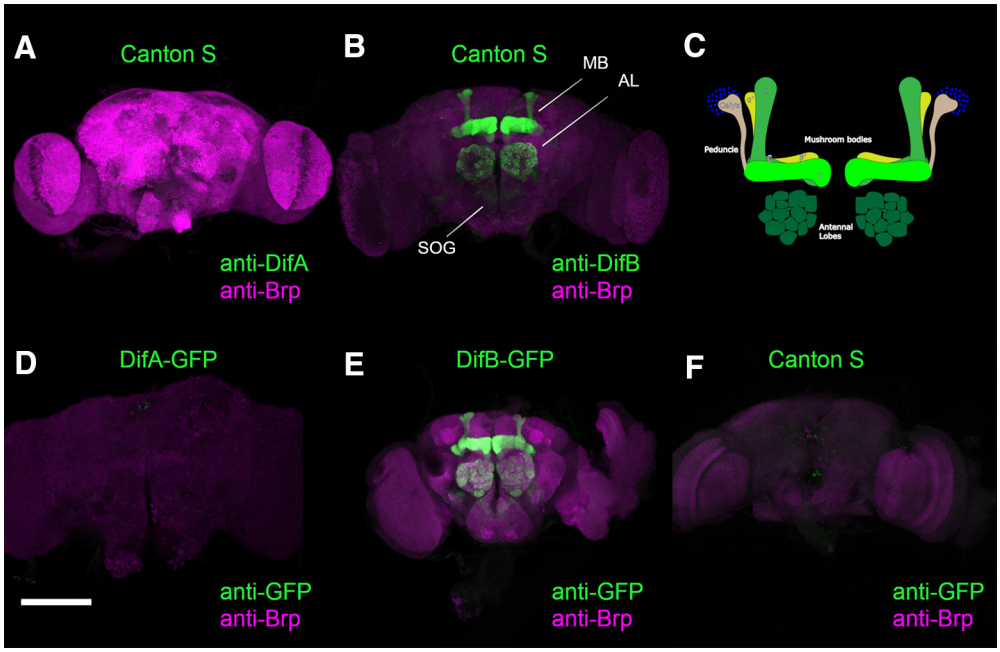

Figure 8. DifB isoform is expressed in the mushroom bodies, antennal lobes, and subesophageal ganglion of the adult brain whereas DifA isoform is not expressed in the brain. ***A***, Immunohistochemical staining with anti-DifA shows no DifA protein expression the adult brain. ***B***, anti-DifB antibody stains neuropil regions of the mushroom bodies, antennal lobes, and subesophageal ganglion of the adult brain. ***C***, Diagram showing relative DifB-positive neural structures. ***D***, CRISPR was used to tag the DifA splice variant with an inframe eGFP cassette. Immunohistochemical staining with anti-GFP shows that the tagged DifA protein is not expressed in the adult brain. ***E***, CRISPR was used to tag the DifB splice variant with an inframe eGFP cassette. Immunohistochemical staining with anti-GFP shows that the tagged DifB protein is expressed in the adult brain in the same pattern as the unmodified wild-type DifB variant (compare to ***B***). ***F***, Anti-GFP immunohistochemical staining shows that wild-type (Canton S) brain does not contain any GFP immunoreactivity. All brains were co-stained with anti-Brp antibody (Brp is a component of the synaptic active zone). Scale bar: 100 μm.

show slight ethanol sensitivity relative to Canton S in the duration of loss-of-righting reflex assay (Fig. 4*C*). The ethanol sensitivity of the DifB mutant allele is recessive (Fig. 5*A*). eGFP-tagging of the DifB protein does not alter ethanol sensitivity (Fig. 5*C*,*D*).

Neither the DifA nor the DifB mutations affect the preference of males or females for consumption of ethanol food in the CAFE assay. However, female DifB mutants did show a reduction in total fluid consumption (Fig. 6).

Tissue-specific expression of the DifA and DifB isoforms

DifA and DifB protein expression patterns were determined using anti-DifA and anti-DifB C-terminal specific antibodies and confirmed using DifA and DifB isoforms that were CRISPR tagged at the carboxy terminus with eGFP. Immunochemical staining of larval fat bodies for DifA and DifB showed that DifA protein is expressed in fat bodies but DifB protein is not (Fig. 7). Anti-GFP staining for an eGFP-tagged DifA splice variant replicated the pattern observed with the anti-DifA antibody (compare Fig. 7*A*,*B*).

Conversely, DifB was only observed in the central nervous system. Immuno-histochemical staining demonstrated that DifB, but not DifA, is expressed in the brain and thoracic ganglion of the central nervous system (Figs. 8-10). In the brain, DifB appears to be strongly expressed in the neurons of the mushroom

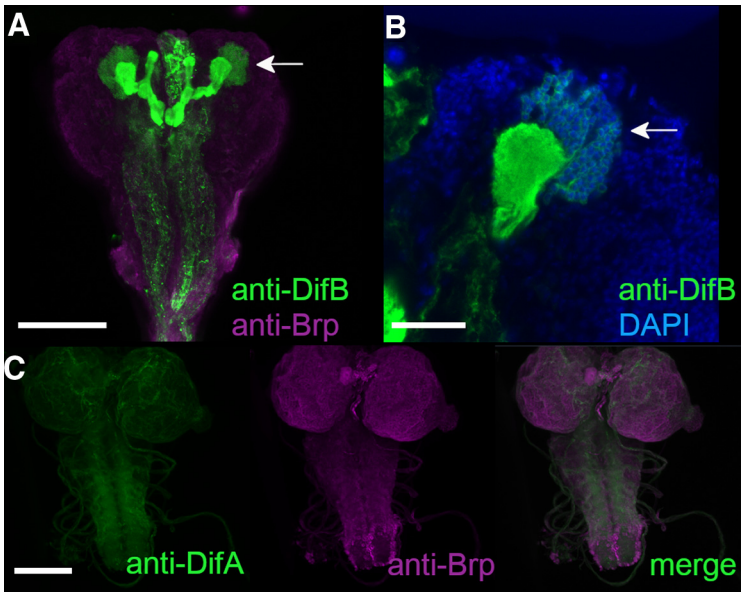

Figure 9. DifB is strongly expressed in the larval brain in the mushroom bodies. ***A***, Staining of the larval brain with anti-DifB shows strong protein accumulation in the neuropil of the mushroom bodies and ventral nerve cord. Brain was co-stained with anti-Brp (Brp is a component of synaptic active zone). Scale bar: 100 μm. ***B***, Close up of the calyx of the larval mushroom body showing that DifB does not colocalize with DAPI-positive nuclei. Scale bar: 25 μm. Arrows identify position of calyx of the mushroom body. ***C***, Anti-DifA does not stain identified structures in the larval brain but instead has a diffuse staining of the larval brain. The merge with anti-Brp co-staining shows that the DifA and neural-specific anti-Brp signals are not coincident. Scale bar: 100 μm. All flies are a Canton S wild-type stock.

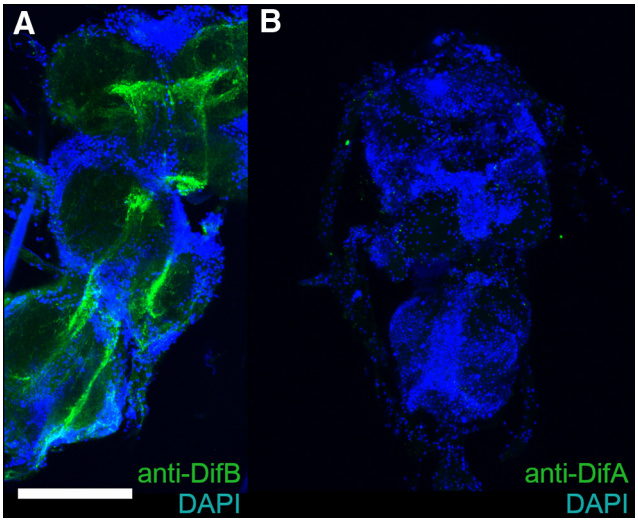

Figure 10. DifB protein and DifA protein localization in adult thoracic ganglion. ***A***, Thoracic ganglion of adult stained with anti-DifB antibody (green) and DAPI (blue). Note that DifB staining is restricted to neuropil regions and does not overlap with DAPI-stained nuclei. ***B***, Adult thoracic ganglion stained with anti-DifA antibody (green) and DAPI (blue). No anti-DifA immunoreactivity is observed. Scale bar: 100 μm. All flies are a Canton S wild-type stock.

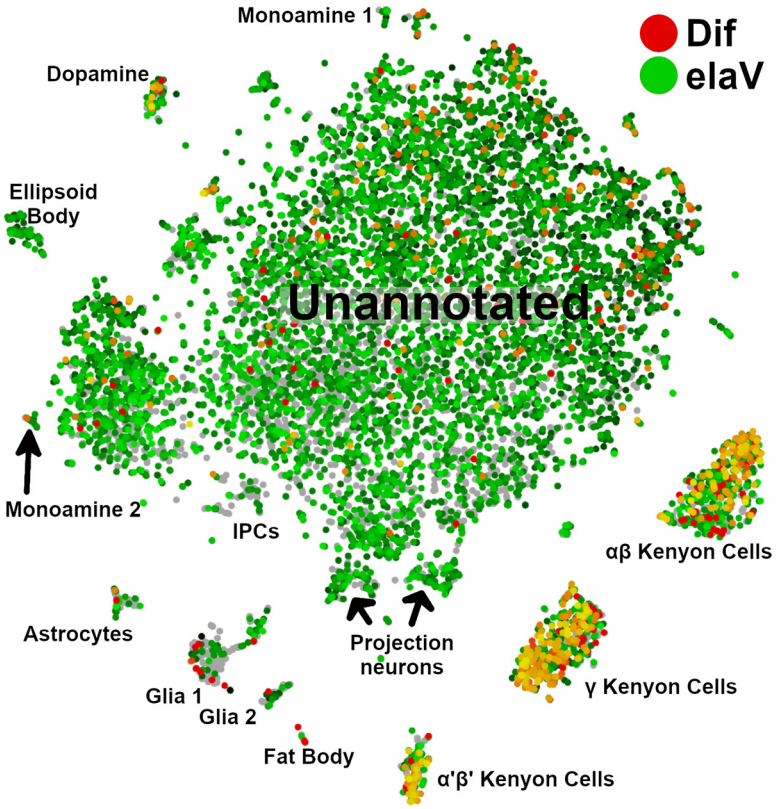

Figure 11. Single-cell transcriptomics confirm that in the adult brain *Dif* is primarily expressed in the mushroom bodies. Cell-type groupings were those identified previously (Croset et al., 2018). SCope visualization of cell type-specific expression of the *Dif* gene in an adult brain preparation (Davie et al., 2018). In this visualization, neurons are marked by expression of the neuron-specific *elaV* gene (green) and *Dif* gene expression is identified by red. Intersection between the *elaV* and *Dif* signals is in yellow. Mushroom body neurons show the majority of overlap between the two signals ($\alpha'\beta'$ Kenyon cells, γ Kenyon cells, and $\alpha\beta$ Kenyon cells; right bottom). Dopaminergic neurons were also enriched for *Dif* expression (left top). Some fat body cells are also *Dif*-positive but this signal does not coincide with the *elaV* signal. The analysis of Croset and colleagues did not distinguish between DifA and DifB isoforms. Naming of clustered groupings are from Croset et al. (2018, their Figure 1). Antennal lobes and subesophageal ganglion were not identified in this analysis.

bodies and antennal lobes (Fig. 8). There is also weak expression in the subesophageal ganglion. We did not observe DifB expression in adult glia (Awasaki and Lee, 2011, compare their Fig. 1 to our Fig. 8) Again, the localization pattern was confirmed using fly lines CRISPR-modified to express DifA-GFP or DifB-GFP. These were stained with anti-GFP antibody (Fig. 8*D*,*E*).

The expression of *Dif* in the adult brain is very similar to the pattern apparent in Drop-Seq single-cell transcriptomic data (Croset et al., 2018). We used the SCope online tool to identify brain regions that express *Dif* transcripts (Davie et al., 2018). This dataset does not differentiate between DifA and DifB splice variants but just generically reports the expression of *Dif* transcripts. Croset et al. (2018) correlated gene expression with specific regions of the brain and associated cells. These data largely support our immunohistochemical observations. In the single-cell transcriptomic dataset, we observed that *Dif* expression is enriched in mushroom body neurons and dopaminergic neurons and sporadically observed in astrocytes and other glia and in fat bodies (Fig. 11). Unfortunately, the antennal lobes fall within the unannotated region of the expression map. Single-cell transcriptomic data also indicate that mushroom body neurons express other components of the Toll signaling pathway (Croset et al., 2018).

The larval brain showed patterns of DifA and DifB expression that were similar but not identical to expression patterns in the adult brain. DifB protein localized to the larval mushroom bodies and to the ventral nerve cord (Fig. 9*A*,*B*). We could not ascertain whether there was expression in the larval antennal lobe and subesophageal ganglion. One difference between adult and larval DifA staining is that there appears to be weak generalized staining by anti-DifA antibody throughout the larval brain whereas the adult brain did not show any DifA immunoreactivity (Figs. 9*C*, 8*A*, respectively).

The DifA mutation and the DifB mutation appear to be highly specific, only affecting expression of their respective products (Fig. 12). The DifB mutation eliminates all DifB immunoreactivity in the adult brain, while the DifA mutation does not appear to affect expression of DifB in the adult brain. We were intrigued by the fact that the DifA mutation eliminates all DifA immunoreactivity in the nuclei of fat bodies, while the membrane-associated immunoreactivity remains (Fig. 12*E*,*G*). Membrane association of a DifA-antibody immunoreactive epitope was also observed in wild type using the anti-DifA antibody and with the eGFP-tagged splice variant stained with anti-GFP (Fig. 7). The annotated Dif splice variants only encode two proteins, DifA and DifB. There are no annotated splice variants that could produce a third non-A, non-B protein variant. This suggests that another *Dif* splice variant that shares the DifA-carboxy terminal region remains to be discovered.

DifB is non-nuclear

While mapping DifB expression in the adult brain, we noticed that DifB staining was restricted to neuropil regions, which are primarily

composed of synaptic connections, and that nuclei were not stained with anti-DifB antibodies (Fig. 13). Adult brains were stained with both anti-DifB and DAPI (to visualize nuclei) and all confocal optical sections viewed for evidence of overlap between DifB immunoreactivity and nuclei (Fig. 14*A*,*B*). No overlap was observed. In addition, colocalization software was used to generate Pearson's correlation coefficients for all images in the Z stacks of brain confocal scans. These showed a negative correlation between DifB and nuclei for both mushroom bodies and antennal lobes (Fig. 14*C*). This absence of overlap is consistent with the idea that DifB is unable to enter the nucleus, an idea that is supported by the observation that splicing of the DifB mRNA omits the NLS (Zhou et al., 2015).

To test the idea that DifB is associated with the synapse but not with the nucleus, we performed a synaptoneurosome preparation from *Drosophila* heads. This preparation generates a nuclei-enriched fraction and a synaptoneurosome-enriched fraction. Synaptoneurosomes consist of composite resealed presynaptic and postsynaptic structures. To determine whether DifB was associating with the nuclei or the synaptoneurosome fraction, we compared the relative abundance of DifB, histone H3 protein, and the Brp protein in each fraction. The histone H3 protein serves as a marker of the nuclei fraction, and Brp protein is a well-characterized presynaptic active zone protein (Wagh et al., 2006). We observed that the DifB protein strongly copurified with Brp and purified away from histone H3 (Fig. 15).

We also asked whether activation of the innate immune system by infection with *B. bassiana* (known to activate Dif; Hedengren-Olcott et al., 2004) would cause DifB to migrate to the nucleus. Infection did not promote nuclear entry (Fig. 14*D–F*), although flies showed an accelerated 10-d mortality profile caused by infection with the fungus.

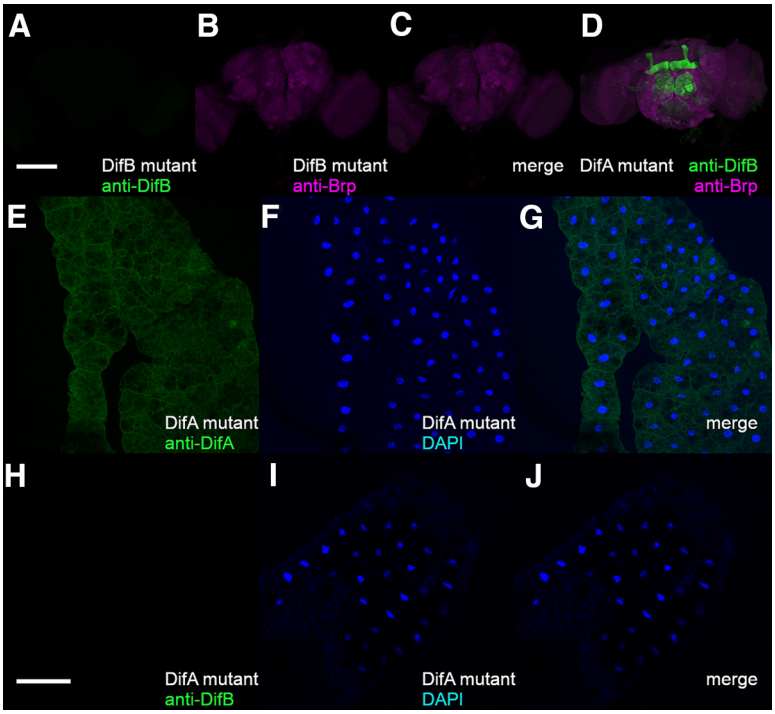

Figure 12. The splice variant specific mutants eliminate expression of their respective products. DifB mutant stained with anti-DifB antibody (***A***), co-stained with anti-Brp (***B***), and the merge of antibody and anti-Brp staining (***C***). DifA mutation does not affect DifB protein localization in the brain (***D***). In larval fat body, the DifA mutation eliminates DifA immunoreactivity in the nuclei (***E***, ***F***). Faint anti-DifA staining localizes to the fat body membrane. Anti-DifA immunoreactivity in ***E***, DAPI staining in ***F***, and merge of the two in ***G***. DifA mutant does not affect staining of anti-DifB in larval fat body (***H***). DAPI staining in ***I*** and merge in ***J***. Scale bars: 100 μm.

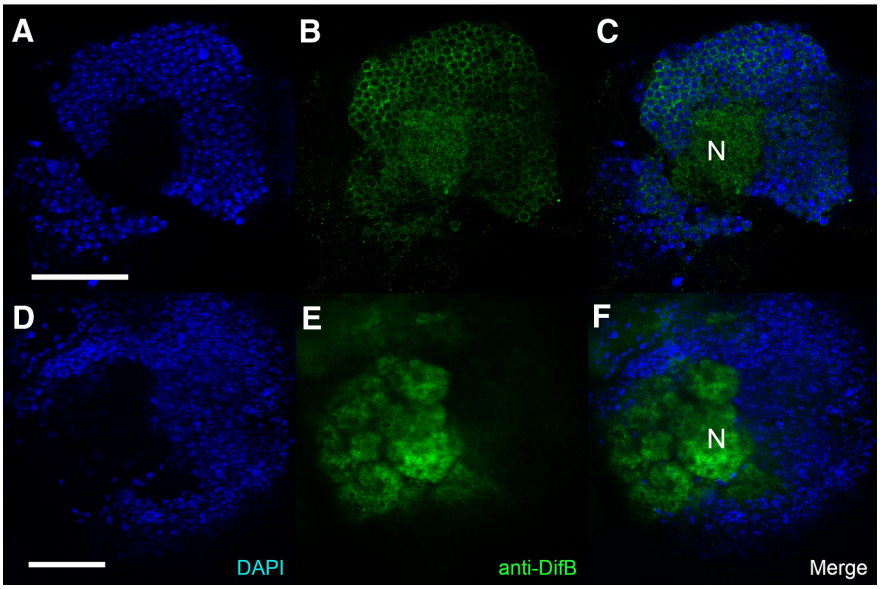

Figure 13. DifB protein localizes to neuropil region. In mushroom bodies, DifB protein localizes to the neuropil region and surrounds the nuclei, while in antennal lobes, DifB protein localizes only to neuropil region and does not surround nuclei. Flies are Canton S wild type. Top row is a mushroom body calyx showing (***A***) DAPI staining for nuclei, (***B***) anti-DifB antibody staining, and (***C***) overlay between DAPI and anti-DifB antibody staining. Notice that anti-DifB staining surrounds nuclei and is found in the neuropil area (N) that lacks nuclei. Bottom row is an antennal lobe showing (***D***) DAPI staining for nuclei, (***E***) anti-DifB antibody staining, and (***F***) overlay between DAPI and anti-DifB antibody staining (N marks neuropil region). Scale bars: 25 μm.

Discussion

In mammals, NF-κB is found in both synapses and dendrites. In hippocampal synaptosomes, NF-κB has been shown to exist in membrane-bound and membrane-free fractions. Synaptic activation can cause this synaptosomal NF-κB to translocate to the nucleus, where it plays roles in learning and in memory consolidation (for review, see Salles et al., 2014).

In *Drosophila*, the phenomenon of non-nuclear localization of an NF-κB was first demonstrated for the *dorsal* (*dl*) NF-κB transcription factor. The *dl* and *Dif* genes are products of a gene duplication and are located ~3.7 kb apart on chromosome 2. The *dl* NF-κB gene is of central importance in the determination of dorsal-ventral polarity during embryogenesis and is an

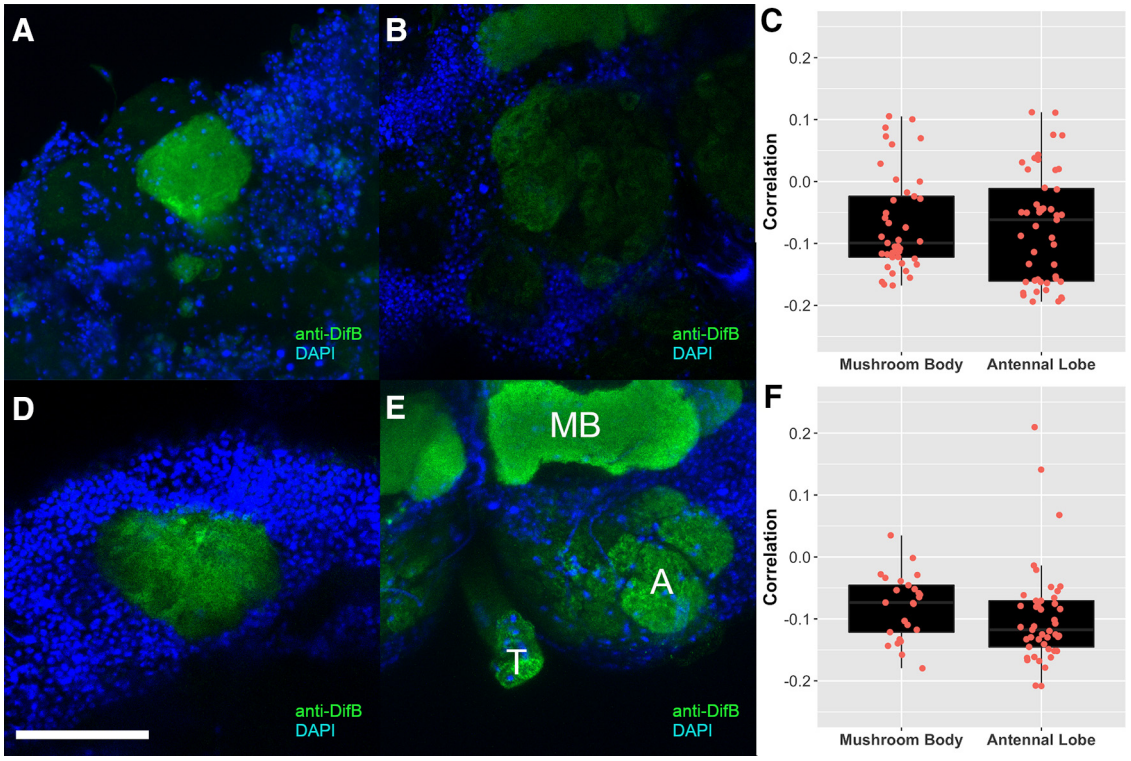

Figure 14. DifB is anti-correlated with nuclei. No overlap between DifB and nuclei was observed in any optical section from an adult brain (flies are Canton S wild type). ***A***, Mushroom body calyx region stained with anti-DifB (green) and nuclei (DAPI staining in blue). Scale bar: 50 μm. ***B***, Antennal lobe stained with anti-DifB (green) and DAPI (blue). ***C***, Pearson's correlation coefficient for all optical sections for the mushroom body and antennal lobe shown in ***A***, ***B***. DifB is anticorrelated with nuclei. $N = 41$ sections for the mushroom body and $n = 47$ sections for the antennal lobe. ***D***, Mushroom body calyx [stained with anti-DifB (green) and DAPI (blue)] from a fly infected with *B. bassiana*. Infection does not cause nuclear localization. ***E***, Antennal lobe [stained with anti-DifB (green) and DAPI (blue)] from a fly infected with *B. bassiana*. Infection does not cause nuclear localization. A = antennal lobe. MB = mushroom body γ lobe. T = tracheal tube that often nonspecifically stains because it traps stain (occasionally seen with all stains). ***F***, Pearson's correlation coefficient for all optical sections for the mushroom body and antennal lobe shown in ***D***, ***E***. DifB is anticorrelated with nuclei. $N = 25$ sections for the infected mushroom body and $n = 46$ sections for the antennal lobe.

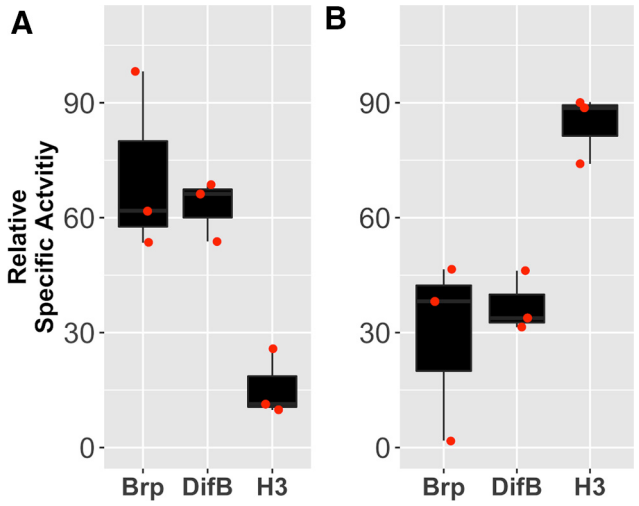

Figure 15. The DifB protein copurifies with a known synaptic protein. Relative abundance of Brp protein (a bona fide synaptic protein), DifB protein, and histone H3 protein (a bona fide nuclear protein) in (***A***) the synaptoneurosome fraction, and (***B***) the crude nuclear fraction. Specific activity of each protein determined by slot blotting using protein-specific antibodies. Specific activity for each protein is expressed normalized to the summed specific activity of both fractions. Brp and DifB purify away from histone H3. Data approximate a normal distribution (Shapiro test) and have equal variance (*F* test), so we used one-way ANOVA $p = 0.0091$ with Dunnett *post hoc* test to test for significance; Brp versus H3 $p = 0.00799$ and DifB versus H3 $p = 0.01668$, $N = 3$. The degree of cross-contamination between fractions is indicated by the relative abundance of histone H3 in the synaptoneurosome fraction and the relative abundance of Brp in the nuclei fraction. All flies are Canton S wild-type flies.

essential gene, whereas the *Dif* gene is not required for normal development and to date has been implicated in only innate immune function. The alternative splicing pattern of *dl* and *Dif* transcripts are very similar. *dl* also produces a B-type splice variant in which the NLS and transactivation domain are replaced by a single large exon. This B-exon encodes a novel amino acid sequence that is 40% identical to the DifB-specific exon (Gross et al., 1999) but for which orthology to other proteins has not yet been recognized.

Heckscher et al. (2007) showed that larval muscle expresses a dorsal protein that does not enter the nucleus but instead surrounds GluRIIA ionotropic receptors at the larval neuromuscular junction (NMJ) and that *dl* loss-of-function mutants reduce the abundance of synaptic GluRIIA and diminish synaptic efficacy (mEPSP depression) without obviously deforming the postsynaptic density. Later, Zhou et al. (2015) showed that the NMJ-specific non-nuclear protein described by Heckscher et al. (2007) was the so-called dorsal-B splice isoform. Because dorsal-B directly modulated synaptic efficacy in larval muscle and because of the similarity in the sequence and organization of the *dl* and *Dif* genes, we asked whether it was the DifB isoform that influenced ethanol sensitivity and whether DifB was excluded from the nucleus. We hypothesize that DifB acts at the synapse to directly modulate synaptic proteins, a hypothesis based on the demonstration that DifB cannot be acting in the nucleus, the similarity between DifB to dorsal-B isoforms, the association of DifB with synaptic regions of the brain, and on the enrichment of DifB in the brain synaptoneurosome fraction. Through such a mechanism, Toll pathway signaling could directly modulate neural activity and behavior.

Direct action of NF-κB on the synapse is a largely unexplored topic and is potentially an extremely fast way for neuroimmune signaling to influence synaptic activity. Recently, the direct modulation of mammalian voltage-gated sodium channels by an NF-κB has been reported (Xie et al., 2019). *Drosophila* appear to have separated nuclear action and nonnuclear action into different NF-κB isoforms that, in the case of Dif, can be individually genetically manipulated. This opens up a new area of neuroimmune signaling for study, the direct and rapid modulation of neural activity by NF-κBs. This area of study may extend beyond an understanding of alcohol and generic sickness responses and may be important for understanding unusual neurologic consequences of neuroimmune activation such as those associated with various mental illnesses and Covid-19 disease (Herron et al., 2018; Iadecola et al., 2020). The fly model system and DifB in particular will be an excellent choice for studying non-nuclear NF-κB effects in isolation from NF-κB action in the nucleus.

We observed that DifB in the adult brain was restricted to neurons of the mushroom bodies and the antennal lobes with very weak expression in the subesophageal ganglion. In addition, we could not find any evidence that DifB enters the nucleus even after stimulation of the Toll pathway by *B. bassiana* infection. Furthermore, immunohistochemical staining and biochemical enrichment of synaptoneurosomes suggest that DifB localizes to synaptic regions. Other fly NF-κB genes have very weak expression in the adult brain (Croset et al., 2018).

In flies and mammals, infection or alcohol exposure evokes signaling through Toll-like pathways that results in the activation of NF-κB proteins and influences alcohol responses (Troutwine et al., 2016; Blednov et al., 2021). The Dif NF-κB is the output of the fly Toll pathway. We hypothesize that Toll signaling bifurcates into an immunity branch that terminates at the DifA isoform and a behavioral branch that terminates at the DifB isoform. In fat body immune cells, Toll pathway signaling would activate only the DifA isoform to transcriptionally stimulate gene expression. In neurons Toll signaling would be restricted to activating the DifB isoform, resulting in changes in behavior, perhaps by directly affecting properties of the synapse.

The hypothesis above should not be interpreted to mean that activation of DifB can have absolutely no consequence for the recovery from infection. We did sometimes observe an almost significant increase in sensitivity to infection in mutant DifB homozygotes (Fig. 2*A*). It may be that under more natural conditions, the behavioral changes evoked by DifB could help avoid succumbing to an infection. While the prerequisite types of changes in behavior could be difficult to detect or even imagine, the following example is instructive. In *Drosophila* larvae, parasitic wasp infection activates the *Dif* NF-κB and increases the preference of larvae for ethanol-rich food. The change in ethanol preference can increase blood ethanol to levels that are toxic to the parasite (Schlenke et al., 2007; Paddibhatla et al., 2010; Milan et al., 2012). This larval response is an exemplar of the surprising ways that complex changes in behavior can help combat infection.

In flies, reducing signaling down the Toll pathway makes animals more ethanol sensitive and increasing signaling makes them more ethanol resistant (Troutwine et al., 2016). This is important because in humans, alcohol insensitivity is associated with increased risk of an AUD (Schuckit, 1994; Heath et al., 1999). The involvement of the innate immune system in modulating alcohol sensitivity means that immune challenges could alter the basal risk of AUD. Furthermore, although TLR signaling through NF-κB transcription factors is known to modulate alcohol responses, the involvement of neural non-nuclear NF-κB in an alcohol behavior is entirely unexplored and would provide a rapid way for Toll-like pathway signaling to modulate alcohol responses.

References

Awasaki T, Lee T (2011) New tools for the analysis of glial cell biology in *Drosophila*. Glia 59:1377–1386.

Beramendi A, Peron S, Megighian A, Reggiani C, Cantera R (2005) The inhibitor kappaB-ortholog cactus is necessary for normal neuromuscular function in *Drosophila melanogaster*. Neuroscience 134:397–406.

Blednov YA, Da Costa A, Mayfield J, Harris RA, Messing RO (2021) Deletion of Tlr3 reduces acute tolerance to alcohol and alcohol consumption in the intermittent access procedure in male mice. Addict Biol 26: e12932.

Caussinus E, Kanca O, Affolter M (2012) Fluorescent fusion protein knockout mediated by anti-GFP nanobody. Nat Struct Mol Biol 19:117–121.

Center for Behavioral Health Statistics and Quality, Substance Abuse and Mental Health Services Administration (2020) Key substance use and mental health indicators in the United States: results from the 2019 national survey on drug use and health. p 114. U.S. Department of Health and Human Services.

Cowmeadow RB, Krishnan HR, Atkinson NS (2005) The slowpoke gene is necessary for rapid ethanol tolerance in *Drosophila*. Alcohol Clin Exp Res 29:1777–1786.

Crews FT, Sarkar DK, Qin L, Zou J, Boyadjieva N, Vetreno RP (2015) Neuroimmune function and the consequences of alcohol exposure. Alcohol Res Curr Rev 37:331–341, 344–351.

Crews FT, Lawrimore CJ, Walter TJ, Coleman LG (2017) The role of neuroimmune signaling in alcoholism. Neuropharmacology 122:56–73.

Croset V, Treiber C, Waddell S (2018) Cellular diversity in the *Drosophila* midbrain revealed by single-cell transcriptomics. Elife 7:e34550.

Davie K, et al. (2018) A single-cell transcriptome atlas of the aging *Drosophila* brain. Cell 174:982–998.e20.

Depner H, Lützkendorf J, Babkir HA, Sigrist SJ, Holt MG (2014) Differential centrifugation–based biochemical fractionation of the *Drosophila* adult CNS. Nat Protoc 9:2796–2808.

Erickson EK, Grantham EK, Warden AS, Harris RA (2019) Neuroimmune signaling in alcohol use disorder. Pharmacol Biochem Behav 177:34–60.

Gratz SJ, Ukken FP, Rubinstein CD, Thiede G, Donohue LK, Cummings AM, O'Connor-Giles KM (2014) Highly specific and efficient CRISPR/Cas9-catalyzed homology-directed repair in *Drosophila*. Genetics 196:961–971.

Gross I, Georgel P, Oertel-Buchheit P, Schnarr M, Reichhart JM (1999) Dorsal-B, a splice variant of the *Drosophila* factor dorsal, is a novel Rel/NF-kappaB transcriptional activator. Gene 228:233–242.

Heath A, Madden P, Bucholz K, Dinwiddie S, Slutske W, Bierut L, Rohrbaugh J, Statham D, Dunne M, Whitfield J, Martin N (1999) Genetic differences in alcohol sensitivity and the inheritance of alcoholism risk. Psychol Med 29:1069–1081.

Heckscher ES, Fetter RD, Marek KW, Albin SD, Davis GW (2007) NF-kappaB, IkappaB, and IRAK control glutamate receptor density at the *Drosophila* NMJ. Neuron 55:859–873.

Hedengren-Olcott M, Olcott MC, Mooney DT, Ekengren S, Geller BL, Taylor BJ (2004) Differential activation of the NF-kappaB-like factors Relish and Dif in *Drosophila melanogaster* by fungi and Gram-positive bacteria. J Biol Chem 279:21121–21127.

Herron JW, Nerurkar L, Cavanagh J (2018) Neuroimmune biomarkers in mental illness. Curr Top Behav Neurosci 40:45–78.

Hoffmann JA (2003) The immune response of *Drosophila*. Nature 426:33–38.

Hoffmann JA, Reichhart JM (2002) *Drosophila* innate immunity: an evolutionary perspective. Nat Immunol 3:121–126.

Iadecola C, Anrather J, Kamel H (2020) Effects of COVID-19 on the nervous system. Cell 183:16–27.e1.

Ip YT, Reach M, Engstrom Y, Kadalayil L, Cai H, González-Crespo S, Tatei K, Levine M (1993) Dif, a dorsal-related gene that mediates an immune response in *Drosophila*. Cell 75:753–763.

Kamp AM, Bidochka MJ (2002) Conidium production by insect pathogenic fungi on commercially available agars. Lett Appl Microbiol 35:74–77.

Khalil S, Jacobson E, Chambers MC, Lazzaro BP (2015) Systemic bacterial infection and immune defense phenotypes in *Drosophila melanogaster*. J Vis Exp (99):e52613.

Lemaitre B, Nicolas E, Michaut L, Reichhart JM, Hoffmann JA (1996) The dorsoventral regulatory gene cassette spätzle/Toll/cactus controls the potent antifungal response in *Drosophila* adults. Cell 86:973–983.

Medzhitov R, Preston-Hurlburt P, Janeway CA (1997) A human homologue of the *Drosophila* Toll protein signals activation of adaptive immunity. Nature 388:394–397.

Milan NF, Kacsoh BZ, Schlenke TA (2012) Alcohol consumption as self-medication against blood-borne parasites in the fruit fly. Curr Biol 22:488–493.

Mokdad AH, Marks JS, Stroup DF, Gerberding JL (2004) Actual causes of death in the United States, 2000. JAMA 291:1238–1245.

Paddibhatla I, Lee MJ, Kalamarz ME, Ferrarese R, Govind S (2010) Role for sumoylation in systemic inflammation and immune homeostasis in *Drosophila* larvae. PLoS Pathog 6:e1001234.

Park A, Tran T, Atkinson NS (2018) Monitoring food preference in *Drosophila* by oligonucleotide tagging. Proc Natl Acad Sci U S A 115:9020–9025.

Pohl JB, Ghezzi A, Lew LK, Robles RB, Cormack L, Atkinson NS (2013) Circadian genes differentially affect tolerance to ethanol in *Drosophila*. Alcohol Clin Exp Res 37:1862–1871.

Ramazani RB, Krishnan HR, Bergeson SE, Atkinson NS (2007) Computer automated movement detection for the analysis of behavior. J Neurosci Methods 162:171–179.

Rutschmann S, Jung AC, Hetru C, Reichhart J-M, Hoffmann JA, Ferrandon D (2000) The Rel protein DIF mediates the antifungal but not the antibacterial host defense in *Drosophila*. Immunity 12:569–580.

Salles A, Romano A, Freudenthal R (2014) Synaptic NF-kappa B pathway in neuronal plasticity and memory. J Physiol Paris 108:256–262.

Schlenke TA, Morales J, Govind S, Clark AG (2007) Contrasting infection strategies in generalist and specialist wasp parasitoids of *Drosophila melanogaster*. PLoS Pathog 3:1486–1501.

Schuckit M (1994) Low level of response to alcohol as a predictor of future alcoholism. Am J Psychiatry 151:184–189.

Shaffer CD, Wuller JM, Elgin SC (1994) Preparation of *Drosophila* nuclei. Methods Cell Biol 44:185–189.

Soumia PS, Krishna R, Jaiswal DK, Verma JP, Yadav J, Singh M (2021) Entomopathogenic microbes for sustainable crop protection: future perspectives. In: Current trends in microbial biotechnology for sustainable agriculture (Yadav AN, Singh J, Singh C, Yadav N, eds), pp 469–497. Singapore: Springer Singapore.

Troutwine BR, Ghezzi A, Pietrzykowski AZ, Atkinson NS (2016) Alcohol resistance in *Drosophila* is modulated by the Toll innate immune pathway. Genes Brain Behav 15:382–394.

Vandenberg JD (1996) Standardized bioassay and screening of *Beauveria bassiana* and *Paecilomyces fumosoroseus* against the Russian wheat aphid (Homoptera: aphididae). J Econ Entomol 89:1418–1423.

Wagh DA, Rasse TM, Asan E, Hofbauer A, Schwenkert I, Dürrbeck H, Buchner S, Dabauvalle MC, Schmidt M, Qin G, Wichmann C, Kittel R, Sigrist SJ, Buchner E (2006) Bruchpilot, a protein with homology to ELKS/CAST, is required for structural integrity and function of synaptic active zones in *Drosophila*. Neuron 49:833–844.

Xie MX, Zhang XL, Xu J, Zeng WA, Li D, Xu T, Pang RP, Ma K, Liu XG (2019) Nuclear factor-kappaB gates Nav1.7 channels in DRG neurons via protein-protein interaction. iScience 19:623–633.

Yin H, Lin H (2014) Chromatin immunoprecipitation assay of Piwi in *Drosophila*. Methods Mol Biol 1093:1–11.

Zhou B, Lindsay S, Wasserman S (2015) Alternative NF-κB isoforms in the *Drosophila* neuromuscular junction and brain. PLoS One 10:e0132793.